INVESTIGATION OF EXTREME RAINFALL EVENTS OVER THE NORTHWEST HIMALAYA REGION USING SATELLITE DATA

VIDHI BHARTI

MARCH, 2015

ITC SUPERVISORS:
Dr. M.C.J. Damen
Dr. Janneke Ettema
Ms. T. A.R. Turkington

IIRS SUPERVISOR:
Ms. Charu Singh

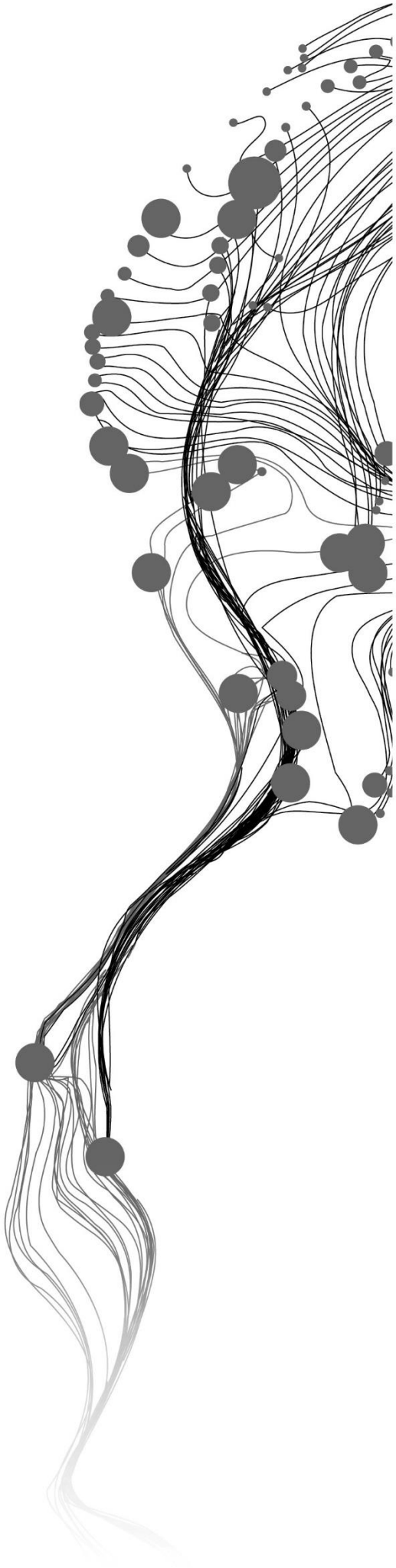

INVESTIGATION OF EXTREME RAINFALL EVENTS OVER THE NORTHWEST HIMALAYA REGION USING SATELLITE DATA

VIDHI BHARTI
Enschede, The Netherlands, [March, 2015]

Thesis submitted to the Faculty of Geo-Information Science and Earth Observation of the University of Twente in partial fulfilment of the requirements for the degree of Master of Science in Geo-information Science and Earth Observation.
Specialization: Natural Hazards and Disaster Risk Management

THESIS ASSESSMENT BOARD:

CHAIRPERSON:	*Prof.dr.ir. M.G. Vosselman*
	Prof.dr. V.G. Jetten
EXTERNAL EXAMINER:	*Dr. Sameer Pokhrel (IITM Pune)*
SUPERVISORS:	*Ms. Charu Singh, IIRS*
	Dr. M.C.J. Damen, ITC
	Dr. Janneke Ettema, ITC
	Ms. T. A.R. Turkington, ITC
OBSERVERS:	
ITC Observer:	*Dr. N. A. S. Hamm*
IIRS Observer:	*Dr. P. K. Champati Ray*

DISCLAIMER

This document describes work undertaken as part of a programme of study at the Faculty of Geo-Information Science and Earth Observation of the University of Twente. All views and opinions expressed therein remain the sole responsibility of the author, and do not necessarily represent those of the Faculty.

Dedicated to my mom

ABSTRACT

Using remotely sensed TRMM 3B42 version 7 precipitation data a thorough investigation of extreme rainfall events during the monsoon season has been conducted over the Northwest Himalaya for the period of 1998 - 2013. The strong positive correlation of 0.88 was found between the TRMM data and ground based IMD gridded rainfall data supporting the use of TRMM satellite data for the study of rainfall over Northwest Himalaya region. However, satellite underestimates precipitation over high mountains of >3000 m elevation and overestimates precipitation over < 3000 m elevation regions. In order to identify the extreme rainfall index three percentiles 98th, 99th and 99.99th of rainfall distribution over the region have been analyzed. It has been shown that the rainfall events exceeding the 99.99th percentile of the region's statistical distribution can be defined as the cloudburst events as the frequency of events decreases steadily with the increasing rainfall intensity. Both Kedarnath (June 2013) and Leh (August 2010) events received rainfall >99.99th percentile of the rainfall distribution of the respective regions. Further it has been observed that spatial distribution of frequency of extreme rainfall events follows the spatial distributions of mean seasonal rainfall and maximum 1-day precipitation. The frequency of extreme rainfall events decreases with increasing elevation. The rainfall intensities associated with 98th, 99th and 99.99th percentiles for each pixel of the Northwest Himalaya shows higher rainfall intensity for the regions with less than 3000 m elevation. Moreover, out of the three states of the Northwest Himalaya, Uttarakhand receives higher frequency of extreme rainfall events with greater intensity than Himachal Pradesh and Jammu & Kashmir. The statistical trend analysis of the frequency of extreme rainfall events using the past 16 years data shows an increasing trend (significant at 1%) of heavy and very heavy rainfall intensity events over the region.

The study of extreme rainfall events in association with the elevation shows that both frequency and intensity of extreme rainfall events typically has an inverse relation with elevation. However, the relation between frequency of events exceeding 99.99th percentile threshold and elevation is not very conclusive. Likewise, the rainfall intensity corresponding to <20 mm day^{-1} and the elevation greater than 3000 m do not correlate well. Furthermore, the plains and the foothills of Northwest Himalaya region with elevation <500 m receive maximum number of extreme rainfall events. However, high frequency of extremes was observed at 1000-2000 m for Uttarakhand and 500-1000 m elevation for Himachal Pradesh. The comparative analysis between Leh and Kedarnath events indicates that Kedarnath disaster was extensive on both spatial and temporal scales covering a vast region for a duration of 3 days from June 15, 2013 to June 17, 2013 whereas Leh cloudburst was a transient localized event. The various atmospheric parameters cloud top temperature, cloud top pressure, cloud fraction and cloud optical depth also give an insight of the prevailing conditions during both the events and may prove helpful in the study of extreme rainfall events in the future.

In the wake of climate change, this study is a contribution in the on-going research of extreme events over mountainous terrain including disaster management study. The sequential remote sensing imageries of rainfall and other atmospheric parameters may be utilized for the now-casting of extreme rainfall events. The present study is supported by the powerful statistical techniques and is also in concordance with the recent similar studies. However, the physical explanation of some of the findings of the present work is beyond the scope of this study. Further, the relationship between topography and rainfall extremes should be studied separately for J&K, Uttarakhand and Himachal Pradesh to get a better insight. This research may also be useful for the modifications in rainfall retrieval algorithms over the mountainous terrain.

Keywords: Extreme rainfall event, Northwest Himalaya, TRMM, elevation

ACKNOWLEDGEMENTS

I take immense pleasure to express my sincere and deep sense of gratitude to my supervising guide, Ms. Charu Singh, who guided me in learning the nuances of research through her immense knowledge, great expertise, sustained enthusiasm, creative suggestions, motivation and exemplary guidance. I could not have imagined a better mentor for my project, for without her towering support, this project would have been left lacking and it would only be pleasing to me to say that the learnings obtained from her will be useful in different stages of my life.

I sincerely acknowledge my ITC supervisors Ms. Thea Turkington, Dr. Janneke Ettema and Dr. M. C. J. Damen for their invaluable feedbacks, continuous support and motivation during the entire phase of my research project, esp. Thea for her continuous encouragement, understanding and insightful comments, which have given me the inspiration to aim higher and work better.

I am grateful to Dr. P. K. Champati Ray, Head, Geoscience and Geo-hazards for his prodigious support, honest opinions and encouragement throughout the course.

I also extend my heartfelt thanks to Dr. N. C. Kingma, Dr. D. B. P. Shrestha, Dr. David Rossiter, Dr. C. J. van Westen and Dr. Nicholas Hamm for their support and valuable discussions, exemplifying the importance of association with ITC, and an immense thanks to the Institute for providing me with such an opportunity.

I offer my profound gratitude towards Dr. Y. V. N. Krishnamurthy, Director, IIRS, Dean Academics (Group Director ER & SS Group) and Dr. D. Mitra, Head, Marine and Atmospheric Science, for providing the facilities to efficiently carry out the project's research in the campus.

Although the project had to be changed from its initially decided subject, I would still like to extend my thanks towards Dr. Richard J. Blakeslee (NASA), Dr. Sherry Harrison (NASA) and Dr. Scott A. Braun (NASA) for their prompt help.

I am also thankful to Mr. Ashish Dhiman for providing help with tasks that may seem trivial, but otherwise would have been unachievable in such a short duration and Mr. Abhishek Das for helping with obtaining the dataset. I am also grateful to the staff, library facilities and Computer Maintenance Department at IIRS and ITC, for their support in various forms.

And last but not the least, I would like to thank my family and friends, for none of this would have been possible without their heartfelt love and untiring support towards me.

TABLE OF CONTENTS

LIST OF FIGURES

LIST OF TABLES

1. INTRODUCTION

1.1. Background

Extreme rainfall events are one of the serious challenges society will have to face with a changing climate. Cloudburst, a ferocious form of extreme rainfall event typically has a potential of causing catastrophic disasters. Colloquially, defined as a sudden copious downpour with a vehement force usually for a very short duration over a restricted region, it is one of the least known mesoscale phenomenon whose physics is not fully understood yet. The Northwest Himalaya (hereafter referred to as NWH) mountain region is highly vulnerable to extreme rainfall events and cloudbursts due to its extremely intricate topography and altitude-dependent climate, consequently leading to sharp weather fluctuations in different sectors of mountains which can be both unpredictable and harsh. This erratic behaviour of the climate leads to sudden occurrences of deluges of short (3-4 h) to long (10-14 h) duration in this orographic region (Nandargi & Dhar 2011). Cloudbursts and associated flash floods are one of the most potent disasters in Himalaya region (Thayyen *et al*. 2013). The NWH has witnessed many colossal disasters initiated by cloudbursts in the recent times causing immense human and economic losses. The Leh cloudburst (August 2010), Kedarnath disaster (June 2013), Rudraprayag cloudburst (September 2012), Manali cloudburst (July 2011) are few of the major cloudburst events notable for causing great damages to human lives and infrastructure. Leh and Kedarnath disasters were one of the most calamitous natural disasters in the history of India. The Kedarnath disaster named 'The Himalayan tsunami' due to the sheer enormity of the scale of the disaster, is acknowledged as India's worst natural disaster since December 2004 tsunami. The Leh disaster was noted to be the worst calamity ever in the Ladakh region as it took roughly 255 lives with 1749 houses destroyed (Thayyen *et al.* 2013 and references therein).

Though the phenomenon is hitting the NWH region severely each year, there has been inadequate research on this subject. Several past studies attempting to study extreme rainfall events over Indian subcontinent largely excluded Himalaya region due to non-availability of data. The remoteness of the Himalaya region, insufficiency of reliable rainfall networks, sparse coverage of rain gauges and Automatic Weather Stations across the mountainous terrain are the major factors responsible for making the prediction and observation of rainfall incredibly difficult in the region. In lieu remote sensing has emerged as an attractive approach to studying precipitation offering high spatial and temporal sampling density unattainable through any other means over complex terrains. The latest advancements in meteorological satellites and improved precipitation estimation algorithms have facilitated the research on such a subject. Tropical Rainfall Measuring Mission (TRMM), a joint mission between The National Aeronautics and Space Administration (NASA) and the Japan Aerospace Exploration Agency (JAXA) was the first satellite primarily dedicated to study rain structure and monitor precipitation distribution over tropics and sub-tropics (NASDA, 2001). TRMM is the only satellite providing inter-calibrated precipitation data routinely since December 1997 at such fine spatial and temporal resolution than any other space-borne precipitation product. Moreover, the latest released version 7 data offers improved precipitation estimations with significantly lower bias even over complex terrain (Huffman *et al*. 2010, Zulkafli *et al.* 2014) making it capable enough not to miss the signatures of extreme rainfall events.

This study aims at studying the extreme rainfall events (hereafter referred to as EREs) in a detailed manner over NWH using TRMM satellite precipitation data. The primary focus is bringing out the probable

locations and examining the spatiotemporal trend of EREs over the study area. Additionally, this research also seeks out the relation between elevation and EREs. A comparative analysis between the Leh and Kedarnath cloudburst disasters has also been carried out which may help delineate the underlying causes and differences between the two case studies. It is noteworthy that this analysis does not aim to explore the physical mechanisms responsible for EREs or orographic precipitation but to provide a framework for identification of probable locations and time of the EREs. It is a contribution in the on-going research on extreme weather events including disaster mitigation study.

1.2. History of Extreme Rainfall Events in the Northwest Himalaya region

It is well known that the Himalaya region has a dominating effect on the Indian summer monsoon but different sections of the Himalaya experience monsoon differently owing to varied topography. The Northeast Himalayan range (not a part of this study) has always been in more focus for research due to its stronger monsoonal capture than the NWH and severe proclivity towards flash floods associated with heavy rainfall. However, the NWH has various similarities and contrasts as compared to the Northeast range of Himalayas, out of which precipitation processes are one of them.

The NWH region is also highly prone to cloudbursts especially the states of Uttarakhand and Himachal Pradesh due to their physiography and heavy rainfall reception during monsoon season as compared to the state of Jammu & Kashmir (Das *et al.* 2006, Kelkar 2007). An ERE alone is not a disaster but acts as an initiator to a number of disasters like flash floods, debris flow, landslides, glacial lake outbursts and lake breach. Commonly, the human and economic losses occur due to post-cloudburst disasters. Howbeit, not all EREs turn into a disaster. The reasons for a cloudburst turning into a disaster include both geographical and anthropological factors. Many cloudburst events go unreported in the remote and unpopulated regions of the Himalayas which hardly pose any threat in terms of human or monetary loss.

A list of major EREs reported as cloudburst events happened in the past has been prepared for each state of the NWH region which brings out the severity of the situation and also highlights the need to study this phenomenon over the region.

Table 1.1: List of major cloudbursts in Himachal Pradesh (source: nidm.gov.in)

Date of ERE	Location
September 29, 1988	Soldang Khad
July 31 – August 2, 1991	Soldang Kahd
September 4-5, 1995	Kullu valley
August 11, 1997	Andhra Khad, Pabbar Valley
July 31 – August 1, 2000	Satluj valley
July 23, 2001	Sainj Valley, Kullu District
July 17-19, 2001	Mandi District
July 29-30, 2001	Chhota Bhangal and Baijnath, Kangra District
August 9-10, 2001	Moral-Danda peak, Shimla district
August 21-22, 2001	Ani sub division, Kullu
July 16, 2003	Kullu district
August 7, 2003	Kullu district
August 15, 2007	Ghanvi, Shimla
August 7, 2009	Dharampur, Mandi
September 12, 2010	Kharahal valley

July 19-20 , 2011	Manali

Table 1.2: List of major cloudbursts in Uttarakhand (source: nidm.gov.in)

Date of ERE	Location
2002	Ketgaon
2004	Ranikhet
July 5-6, 2004	Chamoli
2007	Pithoragarh district
August 6-7, 2009	Pithoragarh district
August 18, 2010	Kapkot, Bageshwar
July 21, 2010	Almora district
September 14-15, 2010	Almora district
August 2-8, 2012	Bhatwari, Uttarkashi
September 13, 2012	Ukhimath, Rudraprayag
June 15-17, 2013	Kedarnath, Pithoragarh
August 1, 2013	Kapkot, Bageshwar

Table 1.3: List of major cloudbursts in Jammu & Kashmir (source: nidm.gov.in and Thayyen *et al*. 2013)

Date of ERE	Location
June 23-24, 2005	Leh Nalla (Ganglass)
July 31 –August 1, 2006	Leh Nalla (Ganglass)
August 5-6, 2010	Leh cloudburst
June 8, 2011	Baggar, Doda

The lists include only those events which were officially recorded and caused human and monetary losses, however many events either go unreported or left merely as an anecdotal record in the local history due to lack of monitoring. Owing to inaccessibility, remoteness and international boundary controversy it has been a challenging task to install rain gauges or radar especially over Jammu & Kashmir (hereafter referred to as J&K). Moreover, the missing information about the exact date and location of many events also draws attention to the lack of proper and systematic documentation of EREs over the NWH region. It can be seen that all these events occurred during monsoon season with the states of Uttarakhand and Himachal Pradesh (hereafter referred to as HP) clearly emerging as highly ERE prone regions. The recent disasters in Leh and Kedarnath due to the large-scale damage and destruction captured the interest of scientific community and also gave rise to a new debate on the destitute state of disaster management in India at both national and regional levels. This work is chiefly motivated by all these factors intending to provide assistance in the field of disaster management over mountainous terrain.

1.3. Research Identification

According to the Intergovernmental Panel on Climate Change (IPCC), the intense and heavy episodic rainfall events are projected to increase in both frequency and intensity with implications for more flooding in the Asian monsoon region (IPCC 2007). As the climate is becoming more extreme in some areas and some variables, there has been a dire need to contemplate & understand weather extremes (Karl and Easterling 1999). However, it depends on our ability to monitor and detect such trends through

effective use of space-based measurements and long-term data assessment. Therefore, this study intends to study EREs using the available long-term satellite precipitation data. Moreover, the ERE lacks any standard definition which allows the introduction of an extreme rainfall index.

The accurate precipitation measurement with the help of appropriate instruments is crucial for the study of EREs. Even though the TRMM precipitation product used in this analysis is a combined microwave-IR estimate with rain-gauge adjustments (Huffman 2013 and references therein), yet errors related to observation, bias, data quality and rainfall retrieval algorithms cannot be refuted. Hence, as rain gauges are the most common and direct method for accurate precipitation measurement, they act as the default source for satellite ground validation.

This study is also an attempt to assess the capability of TRMM version 7 in studying the extremes especially over mountainous region. It can be determined by performing a comparative analysis of two case studies namely Leh and Kedarnath disaster. The Leh cloudburst event was a unique phenomenon owing to Leh's lee side location on the western Himalaya which experiences very little monsoon activity whereas Kedarnath is located on the windward side of the mountains which receives very high precipitation during the monsoon season. The comparison of these two major cloudburst related disasters will give an overview of the leading causes associated with these events.

1.3.1 Research objectives

Based on the problem discussion, the overall quest of this research project can be formulated as follows:

i) To validate the TRMM 3B42 v7 satellite-derived precipitation data with the ground-based IMD rain gauge measurements

ii) To define an extreme rainfall index and extract the spatiotemporal trend and variability of ERE using 16 years of TRMM 3B42 satellite data over the Northwest Himalaya region

iii) To perform the comparative analysis of the two major cloudburst events occurred in recent times *viz.* Leh cloudburst event (August 4-6, 2010) and Kedarnath disaster (June 14-17, 2013)

These objectives pave the way for further investigation. Though both satellite and rain-gauge are gridded datasets, the foremost issue is validating the satellite estimates with ground based precipitation measurements. Testifying satellite precipitation as a reliable mean for studying extremes over mountainous region is a challenge in itself. Furthermore, the limited research conducted over the region presents inconclusive results about the trend of extremes over the NWH region. The Himalayan region is a complex topographic region but the causes of orographic precipitation are also not completely understood by researchers yet. Moreover, topography plays a major role in affecting the orographic rainfall but the relation between elevation and rainfall is poorly defined (Bookhagen and Burbank 2006, Palazzi *et al.* 2013).

1.3.2 Research questions

The following research questions illustrate the aspects of the research objectives pursued:

i) What is the correlation between TRMM satellite-derived precipitation data and ground based precipitation measurements?

ii) Has the frequency and intensity of ERE increased, decreased or remained stagnant over the past 16 years over the Northwest Himalaya?

iii) Is there any association of the elevation with the frequency and intensity of ERE?

iv) What were the differences & similarities in atmospheric conditions and cloud properties between Leh & Kedarnath disasters?

This thesis has been organized into six sections: Chapter 2 summarizes the literature available on extreme precipitation and related factors in mountainous regions. It also elaborates the role of satellites in the measurement of precipitation. Chapter 3 describes the study region from geographical and climatic point of view. Chapter 4 is about the datasets and methodology adopted for this research. Chapter 5 discusses the results obtained. Chapter 6 summarizes the findings, gives conclusions regarding the research objectives and some recommendations for future work on this subject.

2. LITERATURE REVIEW

The Himalayan mountain ranges act as a barrier where a complex interaction between atmosphere and topography takes place which is very challenging to comprehend. Orographic convection due to the diurnal heating and cooling are thought to be responsible for the precipitation over Himalayas which seldom gives rise to flash floods (Chow *et al*. 2013). This chapter briefly discusses the previous studies which explored the topics of orographic precipitation, influence of topography and extreme rainfall events over the Himalaya region.

2.1. Orographic Precipitation

Orographic precipitation is anticipated as the key reason for cloudbursts in mountains as orography influences the formation and movement of localized deep convective systems (Chow *et al*. 2013 and references therein). It can be defined as the modification in the precipitation process due to interaction of moist flow with topography and is considered as one of the most challenging aspects of the mountain environment due to the involvement of dynamics of orographic flow with cloud microphysical processes (Chow *et al.* 2013). The unstable atmospheric layers were believed to be the prime reason along with other meteorological preconditioning like orographic enhancement of existing stratiform rain, forced orographic ascent of existing potential instability and orographic blocking of existing baroclinicity responsible for heavy precipitation on mountains in the classical theory (Paula & Lettenmaier 1994 and references therein, Smith 1982 and references therein). Moreover, orographic precipitation is not only associated with the enhancement of the precipitation at a point but also depletion of rainfall in its absence (Chow *et al.* 2013). One of the prominent example of such orographic effect is windward and leeward precipitation contrast (Shrestha 2000). Whereas due to continuous mechanical uplifting of air mass, precipitation is triggered on windward side at some point, air becomes essentially dry by the time it reaches the leeward side (Anders *et al.* 2006, Paula & Lettenmaier 1994, Smith 1979). In the Himalaya Mountains, Leh region is a good example of such leeward phenomenon acquiring its name 'cold desert'. Commonly, it is highly unusual to encounter an ERE on leeward side. However, understanding orographic factors accountable for precipitation is not that simple.

With the recent advancements in technology, there has been a rapid progress in the understanding of orographic precipitation in a detailed manner. Some argue that topography cannot play a direct role in precipitation processes as lifting alone cannot generate rainfall, therefore orography is just a component of precipitation, not the form of precipitation itself (Barros *et al.* 2004, Houze Jr. 2012, Paula & Lettenmaier 1994). Orographic precipitation has also been assigned as a type in itself due to strong influence of topographic barriers on precipitation processes leading to highly localized rainfall (Sumner 1988). In a comprehensive research study, Houze Jr. (2012) has outlined characteristics of the topography including geometry, height, size, steepness and length of the mountain; microphysical time scales of particle growth and thermodynamics of airflow as basic factors responsible for precipitation fallout. He has further elaborated the mechanisms by which mountains and hills affect the precipitating clouds.

The orographic lifting usually releases the energy of conditional instability resulting in heavy rainfall (Ebtehaj and Foufoula-Georgiou 2010). Another aspect of heavy precipitation in orographic regions is warm rain process. The warm clouds have the ability to achieve a great depth with temperature above than 0° C allowing formation of larger raindrops and make it to the ground as precipitation (Sumner 1988 and references therein). These are the factors responsible for making orographic precipitation processes different than those over the plain regions.

2.2. Role of elevation

Mountainous areas have a strong impact on the spatiotemporal distribution of the rainfall as compared to the plains. The most important mountain characteristic responsible for such distribution of precipitation is elevation. As the altitude increases, the air pressure, temperature and density decreases. The saturation vapor pressure of the atmosphere decreases exponentially with temperature (Khlebnikova 2009). Moreover, there is low portion of fine particles in the air composition. However, establishing a relation between elevation and rainfall considering solely these factors is still not as simple as it seems. This may be due to the distinct geometries and locations of the major mountain ranges around the world.

Barry (2008) identified four primary factors responsible for mountain climates – latitude, continentality, altitude and topography; out of which altitude was regarded as the most fundamental characteristic of the mountain climates. Moreover, altitude and topographic features like slope, aspect and surface exposure to solar radiation altogether create local climate systems within the different sectors of the mountains. Whiteman (2000) attributed terrain height as the primary causative factor but also underscored proximity to moisture sources, terrain relief and aspect relative to the direction of approaching winds as other significant factors affecting spatial variation of precipitation over orographic region. Bookhagen & Strecker (2008) also studied orographic rainfall along South American Andes using TRMM 2B31 & 3B42 datasets and suggested a clear relation between rainfall and topographic relief. They also asserted that topographic relief (elevation difference between maximum and minimum points in a given radius) majorly controls orographic rainfall. The variability in diurnal patterns and annual patterns of relative humidity in mountains is also attributed to the local relief.

Using inhomogeneous rain gauge network distribution Dhar and Rakhecha (1980) brought out the relationship between elevation and average monsoonal rainfall over Central Himalaya which clearly denied any linear relation between both the factors. Instead they proposed a relation of fourth degree polynomial between both factors. They also showed two rainfall maxima, one at foothills and the other between 2000 - 2400 m altitudes. Their research was based on only 50 rainfall stations out of which only 4 were located above 2500 m altitude. Further, Alpert (1986) simulated the distribution of orographic precipitation and came up with 3 rainfall maxima, one at the foothills, second at an elevation of 1500- 2200 m and third at the elevation of about 4000 m.

Several previous studies have also brought out the fact that there is a strong connection between altitude and precipitation, as rainfall usually increases with height only till a certain level, after that it starts decreasing (Shreshta *et al.* 2012, Singh and Kumar 1997). However, elevation alone cannot be held responsible for intense mesoscale orographic rainfall as researchers have always pointed out at the geometry of topography and mountain flows also playing major roles in orographic enhancement of rainfall (Alpert 1986, Anders *et al.* 2006, Paula & Lettenmaier 1994, Smith 1979). However, no study was found which related the elevation with extremes over the NWH region.

2.3. Extreme rainfall event / Cloudburst

The rainfall is a point process with spatiotemporal variability ranging from very weak to extreme within small spatiotemporal scales (Malik *et al.* 2011, Wulf *et al.* 2010). Recently scientists worldwide propose that one of the most serious impacts of global climate change may be the increase in frequency and intensity of extreme precipitation events particularly in mountainous regions (Ghosh *et al.* 2011, IPCC

2007, Joshi & Rajeevan 2006). Based on numerical climate models a global increasing trend in extreme precipitation events is predicted (Hennessey *et al.* 1997, Houghton *et al.* 2001, Sen Roy & Balling Jr 2004). There is no established standard definition of an extreme rainfall event, hence many researchers in the past came up with objective definitions based on the statistical distributions of rainfall at a particular place. The Intergovernmental Panel on Climate Change (IPCC) recognizes an extreme weather event as an event that is rare within its statistical reference distribution at a particular place, usually as rare as or rarer than the 90th percentile. A generic definition identifies it as a transitory localized phenomenon featuring very high intensity rainfall over a restricted region. Nevertheless, researchers have used different thresholds for the identification of EREs. Francis and Gadgil (2006) used 15-20 cm/day as threshold for their study on Indian west coast, Goswami *et al.* (2006) and Rajeevan *et al.* (2008a) defined a 100 mm/day and 150 mm/day rainfall as heavy and very heavy rainfall event respectively for their studies over India using 1° x 1° gridded IMD data whereas Goswami and Ramesh (2007) used 250 mm/day as threshold for the study of extreme rain events over India but they did not include the NWH in their study. Guhathakurta *et al.* (2011) using more than 2599 station data defined 124.5-244.5 mm/day as heavy rainfall and >244.5 mm/day as very heavy rainfall event for their study on ERE over India. Nandargi and Dhar (2012) defined >200 mm/day as heavy rainfall for their study on EREs over northwest Himalaya. They used daily rainfall data for a period of 135 years derived from 150 stations whose elevation vary from 300 m to 4100 m.

Some researchers suggest various statistical methods in order to describe an ERE. The most commonly used is high quantiles of the distribution of precipitation amount e.g. May (2004) used 99th, 99.5th and 99.75th percentiles, Bookhagen (2010) associated 90th and above percentile, Malik *et al.* (2011) used 90th and 94th percentile, Goswami *et al.* (2010) assigned 99th percentile, Krishnamurthy *et al.* (2009) used 90th and 99th percentile as thresholds for a rainfall event to be classified as ERE. However, these thresholds were largely based on the region's climatology which may or may not apply for our study region also. In the guidelines for analyzing extremes, various methods and indices are provided by World Meteorological Organization such as RX1day (maximum one-day precipitation), RX5day (maximum 5-day precipitation), R95pTOT (precipitation due to very wet days >95th percentile), R99pTOT (precipitation due to very wet days >99th percentile) (Klein Tank *et al*. 2009).

In this context, many researchers have attempted to study and analyze the trend and underlying mechanisms responsible for rainfall variability and ERE over the country but rarely including the Himalayas. Sen Roy and Balling Jr (2004) studied trends in extreme daily precipitation over India using seven indices for the period 1910-2000 as obtained from rain gauge data and concluded an increasing trend over the entire country. Ghosh *et al.* (2011) using station data concluded a significantly increasing trend of annual maxima over the country. Joshi and Rajeevan (2006) studied the trend of extreme precipitation using 4 indices over different regions of India with the help of station data. Goswami *et al.* (2006) indicated significantly decreasing trend in moderate events but significantly increasing trend of extreme events over central India during monsoon season. The extreme rainfall events over Indian region have been attributed to monsoon depressions, mid-tropospheric cyclone and active & break spells of monsoon season. However, the results differ due to different thresholds and variations in data used. It is also noteworthy that very few studies were done using remote sensing data. Majority of the studies used coarse resolution data of 1° which may not be competent enough to capture the mesoscale extreme rainfall phenomenon.

2.4. Precipitation study using Remote Sensing

The study of precipitation over Himalaya mountainous region is a challenging task owing to its extremely complex topography and remoteness. There is a serious dearth of adequate reliable rainfall networks in the

region due to difficulty in installation and maintenance of rain gauges and automatic weather stations over the vast expanse of intricate Himalayan range (Anders *et al.* 2006, Basistha *et al.* 2007, Basistha *et al.* 2009, Bookhagen 2010, Singh & Mal 2014). In lieu remote sensing is a pragmatic approach intending to circumvent such issues by offering high spatial and temporal distributions of precipitation (Petty and Krajewski 1997).

The current satellite based techniques for precipitation estimation are more or less indirect measurements. Precipitation estimation techniques predominantly revolve around cloud identification schemes and schemes based on separating raining from non-raining clouds (Kelkar 2007, Kidder & Vonder Haar 1995, Sumner 1988). Current techniques may be divided into 3 categories: (i) Visible and Infra-red (VIS-IR) techniques (ii) Passive microwave techniques (iii) Radar technique. VIS-IR techniques estimate precipitation based on cloud top temperature relate low cloud top temperature as a proxy for rainfall but they do not sense raindrops directly (Kidder & Vonder Haar 1995, Lensky and Levizzani 2008, Petty and Krajewski 1997). This is the reason IR techniques underestimate warm orographic rains (Dinku *et al.* 2008, Li *et al.* 2013). Passive microwave techniques directly sense the precipitation-size drops as high humidity or precipitating clouds result in high microwave emissivity. However, it gives better results over ocean surfaces than land surfaces (Sumner 1988). They are based on either absorption or scattering properties of atmospheric constituents. The major problem is difficulty in separation of cloud water and rain water (Kidder and Vonder Haar 1995). Further, it has been observed that convective rainfall in warm season is usually estimated more accurately by satellites (Li *et al.* 2013 and references therein, Nasrollahi 2015).

TRMM 3B42 v7 is a merged microwave–IR product with rain gauge adjustments produced through improved algorithm and therefore performs better than the previous versions (Huffman 2013 and references therein). Although none of the precipitation estimation technique is free of bias, TRMM 3B42 is reported as having relatively low bias (Smith *et al*. 2006). As the satellite precipitation estimations are indirect measurements, for the accurate precipitation measurement it must be calibrated with ground based observations (Chen *et al*. 2013, Li *et al.* 2013, Smith *et al*. 2006). Even then, the observed differences between both the methods are attributed to the errors in observation, bias and measurements.

2.5. Precipitation in Himalaya region

The Himalaya plays a vital role in maintenance and control of the monsoon system over the entire south Asian region. Huge variations in topography, elevation, soil and rock structures give rise to large climatic variability within small spatial sectors (Pant and Kumar 1997). The Himalaya mountains act as a barrier to intensely cold continental air blowing southwards into the subcontinent during winters and moisture-laden monsoon winds on the southern slopes during monsoon season creating a rain-shadow region in the leeward slopes. The Himalaya mountain range lies in the subtropical high-pressure belt where seasonal meridional migration of pressure and wind systems create variations in seasonal weather.

2.5.1 Precipitation pattern in the Northwest Himalaya

The precipitation pattern in NWH region is controlled by two major atmospheric circulations: Indian summer monsoon (ISM) lasting from June-September and Western disturbances during December to March.

The monsoon is a seasonal reversal of wind – direction and a shift of Inter-Tropical Convergence zone (ITCZ) over north of the equator. Traditionally it is seen as a giant land-sea breeze phenomenon due to differential heating between the Asian land mass and the Indian Ocean (Kelkar 2007). The monsoon

oscillation is stronger in northern hemisphere than southern hemisphere especially over Southeast Asia because of the Himalayas (Kelkar 2007).

The two branches of ISM are, Arabian Sea branch and Bay of Bengal branch. The western Himalaya primarily receives rainfall caused by moist air currents coming from Bay of Bengal which have been deflected westwards after hitting the eastern Himalaya range. The monsoon onset occurs at around first week of July at the foothills (as shown in figure 2.1) of Uttarakhand state. The north-western part of the country is the last to receive the monsoon rains particularly J&K as the monsoon strength decreases from east to west along the path of its travel (Basistha *et al*. 2007). Figure 2.1 shows the normal onset dates of ISM over Indian sub-continent. The Himalaya range forms an orographic barrier by forcing the moist air to ascend and precipitate on the southern slope while hampering the migration of moist air towards northern leeside creating a prominent rain shadow region (Singh & Kumar 1997, Wulf *et al.* 2010). Furthermore, the rainfall decreases westwards due to increasing distance from the moisture source and decreasing strength of the monsoon winds. The normal duration of monsoon season is approximately 122 days starting from June 1st (Das 2002).

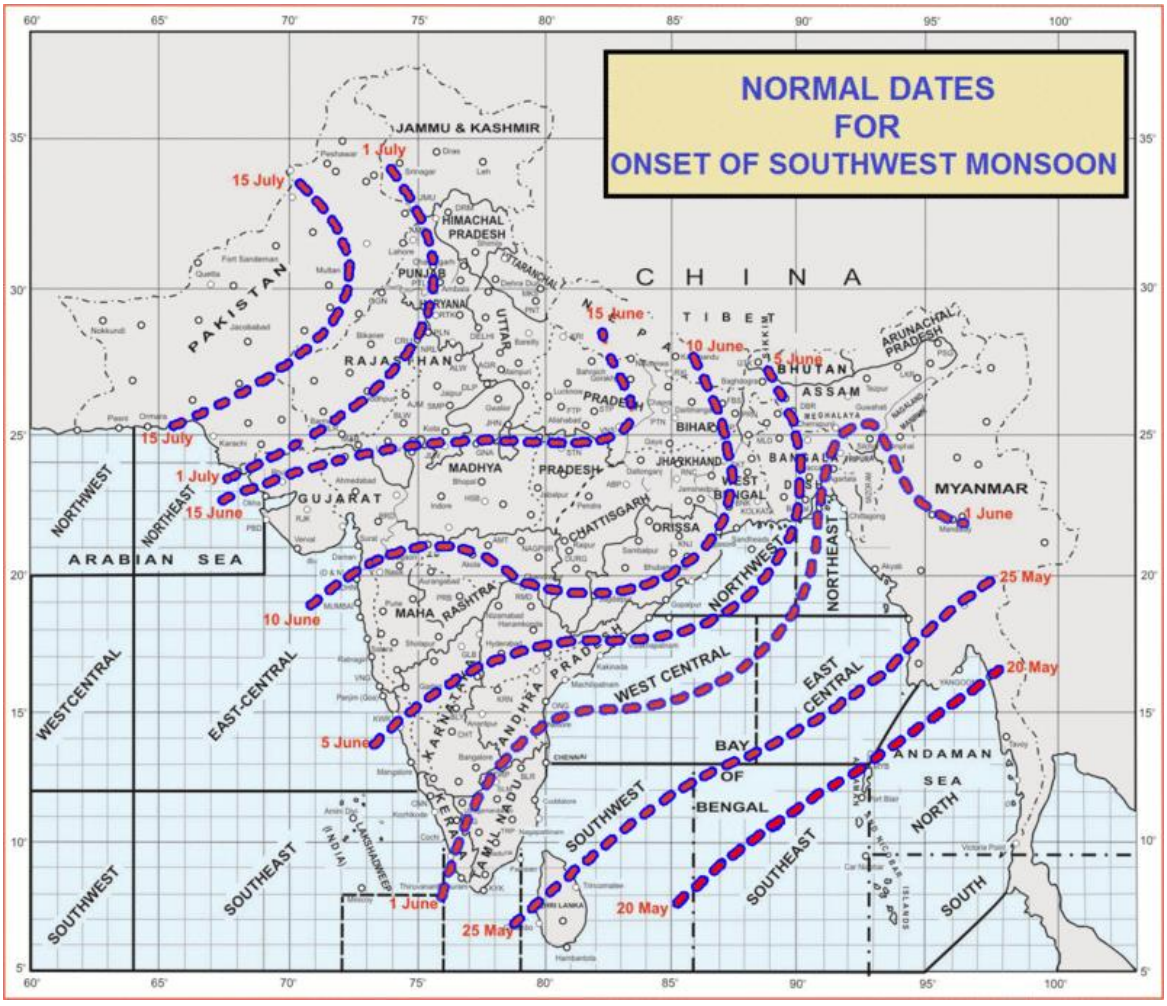

Figure 2.1: Normal dates for onset of Indian Summer Monsoon over Indian subcontinent (source: imd.gov.in)

The strength of the monsoon does not remain uniform throughout the period, instead there are strong intra-seasonal variations known as active and break spells. In the active phase, the most parts of Indian

subcontinent receive good rainfall. These wet spells are interspersed with dry spells or break phase. During these break phases, the axis of the monsoon trough shifts to the foothills of the Himalayas resulting in excess rainfall over NWH while most of the country becomes rainfall deficient (Kelkar 2007, Malik *et al.* 2011, Rajeevan *et al.* 2008b). However, there are no synoptic scale indications for an impending break phase. In general, monsoon starts to withdraw towards the end of the September. Additionally, monsoon is a synoptic scale event and is also influenced by the other large scale phenomena such as El Nino Southern Oscillations and Indian Ocean Dipole (Ashok *et al.* 2001).

During the northern hemispheric winter, low pressure systems originating over the Mediterranean Sea travel all the way to north and northwest India leading to winter precipitation. These migratory systems are known as western disturbance as they enter the country from the west (Pant and Kumar 1997). They are less intense but are capable of reaching higher altitudes in the orogenic interiors resulting in heavy snowfall in Jammu & Kashmir, Himachal Pradesh and Uttarakhand triggering cold waves in north and central India (Wulf *et al.* 2010). These are less intense than convective monsoon rainfall and rarely induce extreme rainfall events. Therefore, only monsoon season has been the focus of this study.

2.5.2 Extreme rainfall events in the Northwest Himalaya

The thermodynamics and orographic uplifting together are considered responsible for extreme rainfall events over the Himalayas (Thayyen *et al*. 2013). However, there has been very limited study on extreme rainfall events over the NWH in the past. Out of which, most of the studies considered the whole 2500 km long Himalaya range for the analysis. Moreover, since eastern Himalaya region receives greater rainfall and experiences floods almost every year, little attention has been paid to the extreme rainfall study over the north-western part of Himalayan range. Singh and Kumar (1997) studied rainfall variations in different ranges of North-western Himalayas in Satluj and Beas basins using station data having limited spatial and temporal resolutions. They observed linearly increase in annual rainfall in middle ranges but exponential decreasing trend with altitude in Greater Himalaya range.

Sen Roy & Balling (2004) studied EREs over the whole India using 129 stations data and generated annual time series of 7 different ERE indices. They reported increase in extreme events in most parts of northwest Himalaya with decrease in some parts of Uttarakhand. In NWH, Himachal Pradesh and Uttarakhand have been reported as particularly prone to cloudbursts due to their steep topography (Das *et al.* 2006). Rakhecha and Soman (1994) studied 1-day, 2-day and 3-day EREs over Indian region using 316 stations with homogeneous and consistent data and pointed out at a decreasing trend for all of them over NWH. Guhathakurta *et al.* 2011 showed a decreasing trend over most of the NWH, however the study was conducted using only a limited number of rain gauges. Sen Roy (2009) studied the trend of EREs using station level hourly precipitation data from 1980 to 2002 and concluded an increasing trend of heavy precipitation events during monsoon season over high altitude regions of NWH including the foothills. A more recent elaborative study by Bhan *et al*. (2015) about Leh 2010 cloudburst event suggests that monsoon does impact rain-shadow regions of Himalaya with enough strength to create flash-flood episodes and orographic features might be contributive towards this recent enhancement of rainfall over Ladakh region.

However, there is a lack of consensus on exact trend as most of the studies were carried out using the coarse resolution or interpolated data over different or limited parts of NWH. Therefore studies at national or regional level show significantly different results. The poor distribution of rain gauges over high elevation ranges have also been a substantial reason for perplexing results about EREs over the NWH.

3. STUDY AREA

The study area is confined to the Northwestern part of the Great Himalaya mountain range extending from 28° N to 37° N and 72° to 82° E encompassing the three states of India - Uttarakhand, Himachal Pradesh and Jammu & Kashmir as shown in figure 3.1. The altitude ranges from 170 m to 7861 m containing some of the World's highest peaks. Geologically, the Himalayan mountain range can be divided into three major fold axes: the Outer Himalaya, the Lesser Himalaya, the Greater Himalaya (Pant and Kumar 1997). The figure 3.1 shows the location of Northwestern Himalayan (NWH) range on Indian subcontinent and the elevation map depicts the topographical variability of the region. This chapter also discusses the geography of Leh and Kedarnath areas which are located in the NWH region. The figure 3.3 shows the location of Leh and Kedarnath regions in the NWH. Leh town is situated in Ladakh district of the state of Jammu & Kashmir whereas Kedarnath town located in Rudraprayag district of Uttarakhand state.

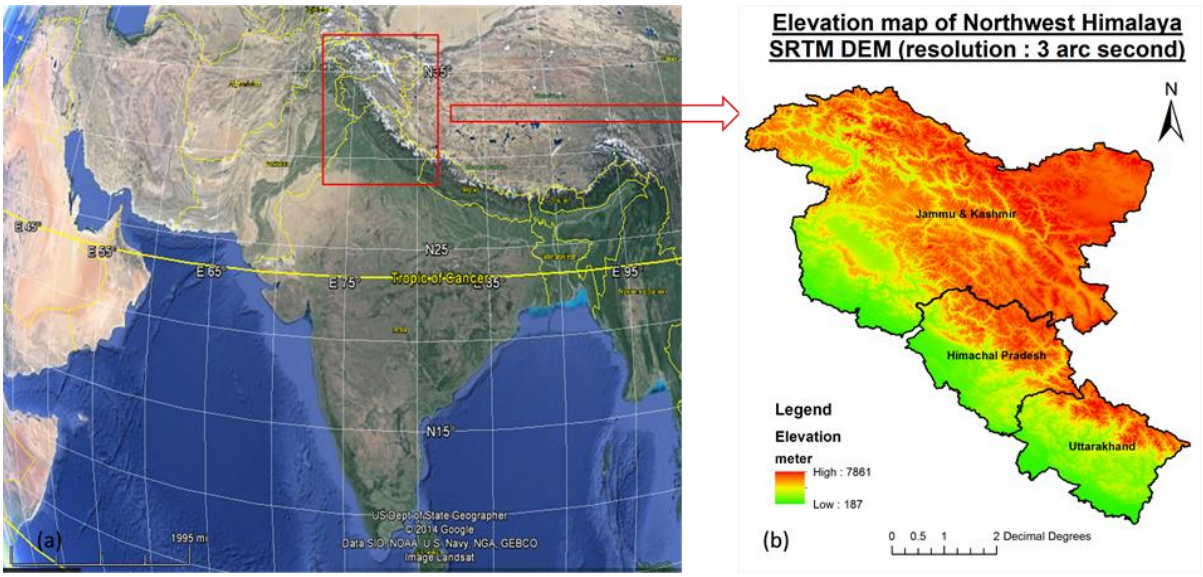

Figure 3.1: Location of (a) Northwest Himalaya on the map of India (source: Google Earth) (b) the states of Uttarakhand, Himachal Pradesh and Jammu & Kashmir in Northwest Himalaya region

According to the altitude, the NWH can be divided into 7 micro climatic zones based on the altitude:

Table 3.1: Climate zones based on altitudes (source: Das 2013 and references therein)

Climate Zones	Altitudes (meter)
Tropical zone	300 - 900
Warm temperate zone	900 - 1800
Cool temperate zone	1800 - 2400
Cold zone	2400 - 3000
Alpine zone	3000 - 4000
Glacial zone	4000 – 4800
Perpetually frozen zone	> 4800

3.1. Overview of the Northwest Himalaya

Though all three states have huge topographic variations, their climatology differ in various aspects. IMD has produced a list of rainfall zones based on the altitude given in Table 3.2:

Table 3.2: Rainfall zone classification based on altitude produced by IMD

Altitude	Rainfall (cm)	Physiography
>3000	Less than 100 to 200	Very very steep side slope (>50%)
2000 - 3000	200 – 300	Very very steep side slope (>50%)
1000 - 2000	200 to 300 or more	Very steep side slope (33-50%)
<1000	Less than 200 to 300	Steep side slope (15-33%)

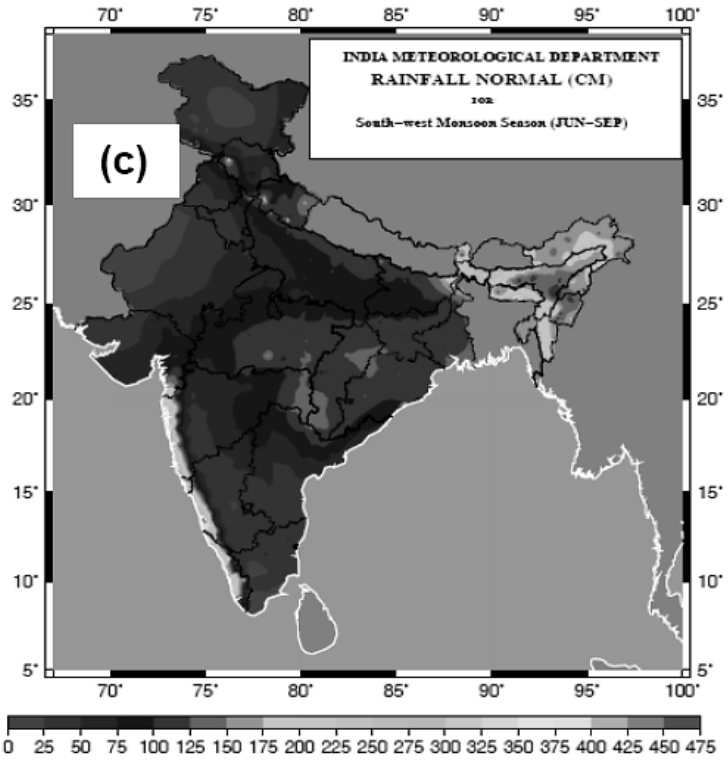

Figure 3.2: Normal rainfall pattern during Southwest monsoon over India (source: Attri & Tyagi 2010)

The map given in figure 3.2 depicts the normal rainfall pattern over the whole country during summer monsoon season. One can easily notice the very low rainfall region over J&K in the figure 3.2. The few regions having high rainfall of around 200 cm can be seen in NWH region, mainly located in Uttarakhand and Himachal Pradesh. The study region has been further divided into three states for better regional analysis. The brief description for each state is given below:

3.1.1 Uttarakhand

Uttarakhand state extends from 28°43` to 31°27` latitude and 77° 34` to 81°02` longitude with altitude ranging from 175m to 7409 m (GTOPO30 Digital Elevation Data) above mean sea level and average annual rainfall of approximately 1494.72 mm (www.imd.gov.in/section/hydro/distrainfall/webrain/uttarakhand). The state has an area of 53485 km^2

and 9 out of its 13 districts have elevation above 2000 m. Geologically, the state can be divided into four major regions: Terai and Bhabar (175-600 m), Shivalik (600-1200 m), Lesser Himalaya (1200-3000 m) and Greater Himalaya (3000-7000 m) (Chopra 2014). Due to extreme topographic variability, the state experiences climate ranging from sub-tropical and sub-tundra.

3.1.2 Himachal Pradesh

The alpine state of Himachal Pradesh extends from 30° 20` 40`` to 33° 12` 20`` N and 75° 30` 55`` to 79° 04` 20`` E covering the area of 55,673 km² (Himachal Pradesh Development Report). The elevation ranges from 250 m to 6475 m above mean sea level and experiences average annual rainfall of approximately 1178.23 mm/year (www.imd.gov.in/section/hydro/distrainfall/hp.html). Geologically, it can be divided into three zones: (i) Outer Himalayas (up to 1500 m) (ii) Inner Himalayas (up to 4500 m) (iii) The greater Himalayas (above 4500 m). Having such a distinct topographic ruggedness, it experiences altitude-dependent climatic variability ranging from semi-tropical to semi-arctic. The state has three seasons – rainy season (June – September), winter season (October – March) and summer season (April – June) (Planning Commission HP).

3.1.3 Jammu & Kashmir

The northernmost state of India, Jammu and Kashmir (J&K) lies between 32° 17` N to 36° 58` N latitude and 73° 26` E to 80° 30` E longitude covering the area of 222 236 km². The territories of Jammu, Kashmir, Ladakh and Gilgit form the state of J&K. The whole state comprises of complexly folded young mountain systems with elevation ranging from 290 m to above 7000m. Altitude and prevailing winds contribute in distinct variations in climatic conditions (Raina 1971). The range of climatic conditions vary from sub-tropical heat of Jammu to semi-Arctic cold of Ladakh. Although the average annual rainfall of J&K is 785.86 mm/year (http://www.imd.gov.in/section/hydro/distrainfall/jk.html), there is immense rainfall variability within the state as Jammu district receives up to 1200 mm average annual rainfall as compared to Ladakh district which receives approximately 45 mm annual rainfall.

3.2. Overview of Leh and Kedarnath

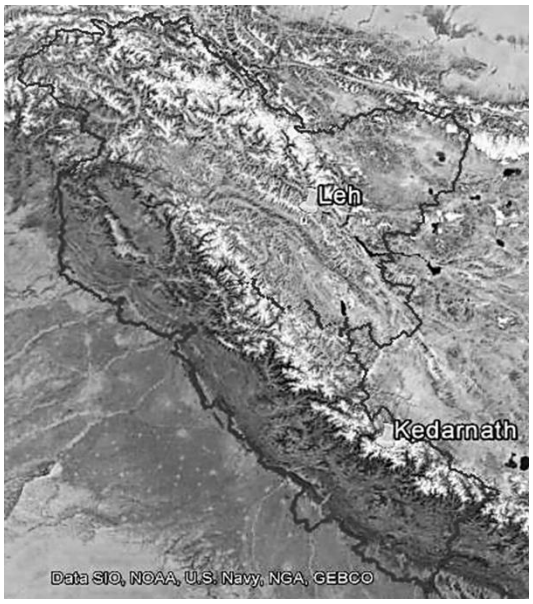

Figure 3.3: Location of Leh and Kedarnath in the Northwest Himalaya region (Source: Google Earth)

Leh is the main town of Ladakh district situated at approximately 34°09` N latitude and 77° 34` E longitude located at approximately 3500 m above mean sea level. The whole district is extremely mountainous with three parallel Himalayan ranges – Zanskar, Ladakh and Karakoram Range (Leh.nic.in). Leh has cold arctic desert like climate with wide diurnal and seasonal temperature fluctuations ranging from -40° C in winter to 35° C in summer. Situated on the leeward side of the Himalayan region, it receives very low precipitation approximately 45 mm annually which is mainly in the form of snow. Air is very dry and relative humidity ranges from 6-24 % (Pant and Kumar 1997).

Kedarnath is a small town situated in Rudraprayag district with coordinates 30° 44' N and 79° 04` E in the Mandakini river valley at approximately 3500 m elevation. It is situation on the outwash plane of Chorabari and other glaciers (Dobhal *et al*. 2013). As contrast to Leh, the area receives heavy rainfall during monsoon season primarily in July and August due to its windward location and snowfall in winters due to western disturbances.

4. DATASETS AND METHODOLOGY

Remotely sensed data in conjunction with ground based observations has been utilized in the present study in order to obtain more accurate precipitation values. This chapter covers the datasets and the applied methodology in detail.

4.1. Satellite Data Utilized

Different remote sensing datasets have been utilized to obtain rainfall, elevation and atmospheric variables. The individual datasets and the initial pre-processing has been detailed below.

4.1.1 TRMM 3B42 v7 dataset

The precipitation data has been obtained from Tropical Rainfall Measuring Mission, an international project of NASA and JAXA designed to primarily observe rain structure, rate and distribution in tropical and sub-tropical regions. TRMM was the first ever satellite mission dedicated to measuring rainfall in order to understand global climate system (NASDA, 2001).

The 3-hourly combined microwave-IR estimates (with gauge adjustment) product 3B42 from '*TRMM and Other Precipitation Data set*' data inventory is utilized in the analysis. The algorithm 3B42 produces precipitation by merging high quality (HQ)/infrared (IR) precipitation and root-mean-square (RMS) precipitation-error estimates (Huffman 2013 and references therein). The precipitation data is available in gridded format with 3-hour temporal resolution and 0.25° x 0.25° spatial resolution extending globally from 50° south to 50° north latitude. This dataset is available for the period January 1998 – present. It is noteworthy that version 7 is considered as a huge improvement over previous versions particularly at some specific regions including Himalayan foothills and is recommended for research work (Huffman and Bolvin 2014).

The TRMM 3B42 v7 (hereafter referred to as TRMM data) has been prepared using high quality (HQ) microwave estimates which are calibrated and combined and then used in generation of variable rain rate (VAR) infrared estimates; followed by combining both the estimates and providing the 'best' estimate of precipitation in each grid box at each observation time. Further, the algorithm uses rain gauges indirectly to rescale the estimates to monthly data (Huffman 2013 and references therein). HQ and VAR estimates are summed over a calendar month to create a monthly multi-satellite (MS) product. MS and rain gauge data are further combined to create a monthly satellite-gauge combination (SG). The field of ratios SG/MS is calculated and applied to scale each 3-hourly field in the month (Huffman 2013 and references therein).

The downloaded data comes as 8 time-step files corresponding to 00, 03, 06, 09, 12, 15, 18 and 21 GMT for each day of the year. Each 3-hour archived dataset is in the format of Hierarchical Data Files (HDF) which comes along with metadata file attached with each HDF file. Each HDF file contains 'precipitation' variable (along with other variables) which has precipitation estimates in a 0.25° x 0.25° (cylindrical equidistant) gridded array format. The values of precipitation are 3-hourly average centred at the middle of each 3-hour period with unit mm/h. (For more details please refer to http://disc.sci.gsfc.nasa.gov/additional/faq/precipitation_faq.shtml). The precipitation here refers to all kinds of precipitation either in liquid or solid form. The archived 3B42 dataset is provided by the Goddard Earth Sciences (GES) Data and Information Services Centre (DISC). TRMM Online Visualization and Analysis System (TOVAS), a part of the Giovanni (GES-DISC Interactive Online Visualization ANd aNalysis Infrastructure) web application has been utilized in order to generate the spatial plots of 3-hourly precipitation for the comparative analysis between Kedarnath and Leh events.

4.1.2 SRTM DEM

For the elevation data, NASA's Shuttle Radar Topography Mission (SRTM) generated Digital Elevation Model (DEM) version 4 having spatial resolution of 3 arc second (~90 m) has been used. The version 4 product has been developed using new interpolation algorithms and better auxiliary DEMs. The vertical error is reported to be less than 16 m (http://srtm.csi.cgiar.org/). The data comes in GeoTiff format and has been downloaded from the website of The CGIAR Consortium for Spatial Information (CGIAR-CSI).

The reason behind using SRTM DEM for elevation data is that it is an extremely accurate global elevation model with vertical accuracy of 6 m and horizontal pixel spacing of 30 m developed using single-pass radar interferometry (Jarvis *et al.* 2004). Further, in a detailed quality, accuracy and usability assessment of SRTM DEM using several case studies Jarvis *et al.* (2004) have concluded that SRTM DEM provided more accurate elevation and terrain derivatives than TOPO DEMs, especially for coarse resolution TOPO DEMs.

4.1.3 MODIS Terra and Aqua Daily Level-3 data

The atmospheric parameters being examined in the comparative analysis are the products of MODIS (Moderate - resolution Imaging Spectroradiometer) onboard Terra and Aqua satellites. The Level-3 MODIS Atmosphere Daily Global Product has been derived from 80 scientific parameters from four Level-2 MODIS atmospheric products - Aerosol, Water Vapor, Cloud and Atmosphere Profile. The two MODIS Daily global data product files are one which collected from Terra platform and another collected from Aqua platform. A range of statistical parameters are computed and sorted into 1° x 1° equal angle grid cells that span a 24-hour (00 – 24 GMT) interval (Hubanks *et al.* 2008). For more details please refer to Hubanks *et al.* (2008).

In this study, Aqua and Terra products have been utilized for the comparative analysis between Leh and Kedarnath respectively. The satellite with better overpass during the event has been chosen. This data has been accessed through Giovanni (**G**eospatial **I**nteractive **O**nline **V**isualization **AN**d a**N**alysis **I**nfrastructure) - Interactive Visualization and Analysis , a web- based application developed by NASA's Goddard Earth Sciences Data and Information Services Center (GES DISC). Through this portal, the atmospheric daily global version 5.1 data has been used for the study. The atmospheric parameters and cloud properties that are used for the comparative analysis are mentioned in the following paragraph (http://disc.sci.gsfc.nasa.gov/giovanni/additional/users-manual/G3_manual_Chapter_8_MOVAS.shtml):

i) Cloud top temperature (CTT)

It is the atmospheric temperature at the level of the cloud top. The plots for cloud top temperature have been generated for day and night only. The unit is in degree kelvin.

ii) Cloud top pressure (CTP)

It is defined as the atmospheric pressure at the level of the top of cloud. The plots for cloud top pressure have been studied for day and night only. The unit is in hectoPascal (hPa).

iii) Cloud fraction

It is defined as the fractional area which is covered by the cloud as seen by the satellite from above. It is calculated by dividing the number of cloud pixels by total number of pixels. The plots for cloud fraction have been included for day and night only.

iv) Cloud optical depth (COD)

It is the measure of attenuation of light which has been scattered or absorbed due to cloud droplets. The optical depth or optical thickness is defined as the integrated extinction coefficient over a vertical column of unit cross section.

4.2. Ground validation data

Newly released, high resolution (0.25° x 0.25°) gridded daily rainfall dataset prepared and provided by Indian Meteorological Department (IMD) will be used for the purpose of validation of TRMM 3B42 v7 3-hourly precipitation estimates. This data has been prepared using 6995 rain gauge stations in India (highest number of stations ever used) covering a period of 1901-2013 (113 years). The spatial rainfall distribution in heavy rainfall areas and orographic regions are better presented in IMD4 (hereafter referred to as IMD data) due to higher spatial resolution and rainfall station density (Pai *et al.* 2014).

The standard quality control checks for typing and coding errors, missing data, duplicate station check, extreme value check etc. have been applied after the verification of the location information of the station and typographic errors. The simplest form of inverse distance weighted interpolation (IDW) scheme including directional effects and barriers as proposed by Shepard (1968) has been used for conversion of rainfall station data into grid point data. For the detailed description about the quality control procedures for the preparation of this data set - please refer Pai *et al.* (2014). For this study, the data has been extracted exclusively for monsoon months (June, July, August, September) from 1998-2013 for the Northwest Himalaya region.

4.3. Software used

i) ***Python***: All the initial data extraction and file handling has been done with the help of scripts written in Python programming language using Enthought Canopy version 2.7.3, a cross-platform environment for scientific data computing and analysis.

ii) ***7-Zip***: The TRMM archived data was extracted using 7-Zip File Manager software Copyright (c) 1999-2010 Igor Pavlov.

iii) ***MATLAB***: Developed by The Mathworks Ltd, a fourth generation high-level programming language along with interactive environment is used extensively for scientific data analysis. It has been thoroughly used in carrying out all the data analysis and generation of plots in this project.

iv) ***ArcGIS***: ESRI's ArcGIS is a famous platform for working with maps and spatial information. The maps in the project have been generated using ArcGIS software.

4.4. Research Methodology

The main purpose of this research is to identify extreme rainfall events and examine their trend over the region. Further the relation of EREs with elevation and a comparative analysis between two major EREs occurred in the recent past i.e. Leh and Kedarnath disasters will also be studied. This methodology is partially built on the previous similar research conducted by Bookhagen (2010) and Bookhagen & Burbank (2010). The data validation methodology is inspired from Tawde & Singh (2014). In order to fulfil the discussed purposes, the following approach has been devised as depicted in the diagram:

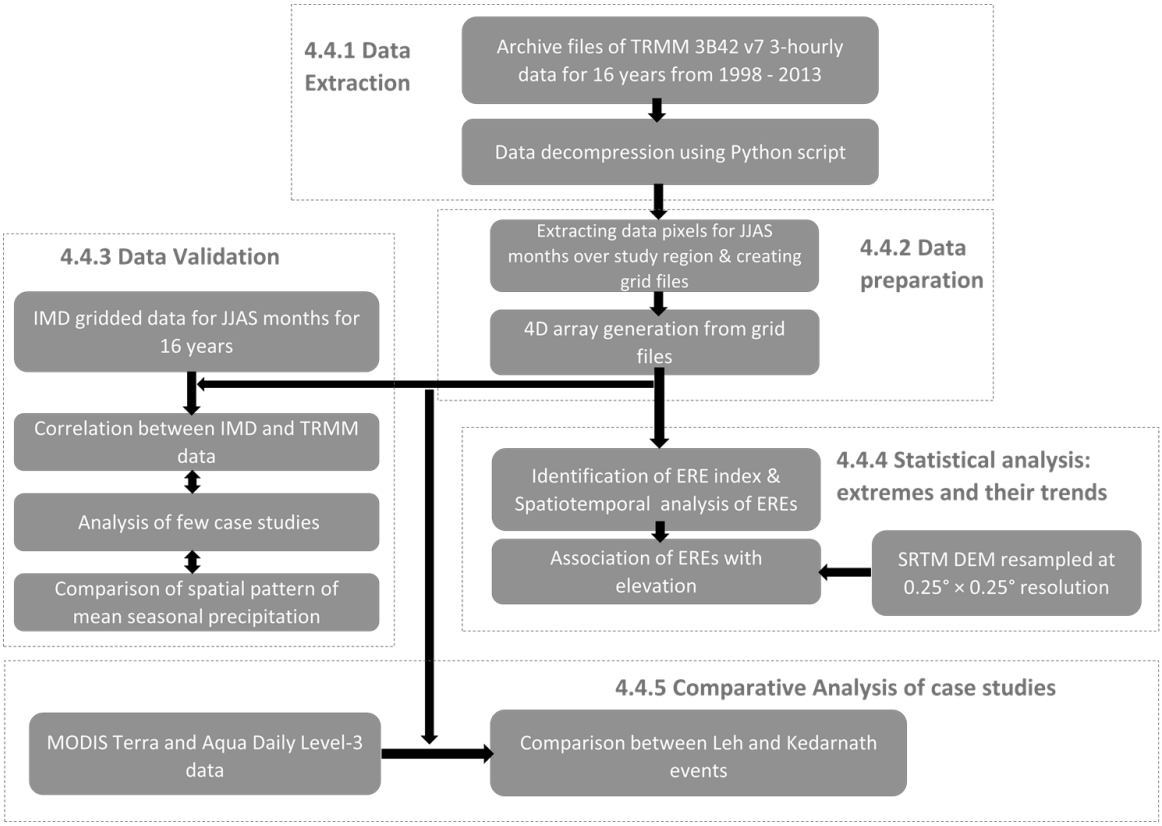

Figure 4.1: Research methodology adopted for this study. The number represents the section where the steps are described in detail.

4.4.1 Data extraction

Roughly 46700 HDF files containing precipitation data were downloaded which came in the form of archived files. A python script was developed to extract all the files to their respective directories. Another python script was generated to create a file list in text format containing precise location of each file for further processing ease (Refer Appendix I for the detailed programs).

4.4.2 Data Preparation

The 8 time-step files initially came in HDF format which were then converted into binary gridded files containing accumulated 3-hour rainfall. The files were extracted only for JJAS (June, July, August, September) i.e. monsoon months for the past 16 years corresponding to the states of Uttarakhand, Himachal Pradesh and Jammu & Kashmir separately and NWH as a whole.

The SRTM DEM data is first extracted for the study region and then resampled from 3 arc second resolution to 0.25° resolution in order to match the spatial resolution of TRMM data. The original DEM had many no-data regions particularly over mountainous terrains including Himalayas. As processed by NASA and USGS, the hole-filling algorithms were applied to provide continuous elevation values (http://srtm.csi.cgiar.org/).

4.4.3 Data validation

It is shown in the previous studies that TRMM 3B42 data gives more accurate precipitation estimates over ocean than land (Chen *et al.* 2013 and references therein). There are also some known deficiencies in the TRMM 3B42 data. The notable deficiencies are the poor correlation between IR brightness temperature and precipitation, variations in coverage of microwave estimates and 3-5% higher microwave estimates than the TRMM 2B31 which serves as a calibrator (Chen *et al.* 2013, Huffman 2013). Therefore, the first

objective of this study is to validate the data with ground-based precipitation measurements for the research work. In order to achieve the objective the following quantitative and qualitative analysis has been performed:

i) Correlation analysis

The correlation analysis has been performed to determine the bias in TRMM dataset with respect to IMD data using Karl Pearson's coefficient of correlation and scatter plot. The Pearson's coefficient of correlation denoted as r, can be calculated using the following mathematical expression:

$$r = \frac{\sum xy}{N\,\sigma_x\,\sigma_y}$$

Where $x = X - \bar{X}$; $y = Y - \bar{Y}$

σ_x = standard deviation of series X

σ_y = standard deviation of series Y

N = number of pairs of observations

ii) Analysis of few case studies

In order to check the potential of the TRMM satellite to capture the extreme rainfall events, a list of cloudburst events occurred in the past was prepared and the comparison of the rainfall registered was performed between IMD and TRMM data.

iii) Comparison of spatial pattern of mean seasonal precipitation

The maps for mean seasonal precipitation using 16 years of data over NWH were generated using both TRMM and IMD data for visual analysis. The rainfall bias for seasonal rainfall at each grid was calculated as:

Rainfall bias = spatial pattern of mean seasonal precipitation (IMD rainfall – TRMM 3B42 rainfall)

The calculated rainfall bias is then compared with the elevation map of the NWH region. This facilitates in distinguishing the elevation ranges where the satellite is overestimating or underestimating the precipitation amount.

4.4.4 Statistical Data analysis : Analysis of extremes and trend analysis

The World Meteorological Organization provides guidelines on analysis of extremes related to weather elements that are measured on daily basis. The guidelines focus only on those weather extremes that are rare within the statistical reference distribution of particular weather elements at a particular place whether or not they turn into an environmental disaster (refer Klein Tank *et al*. 2009).

As rainfall is highly variable phenomenon on spatiotemporal scales, the threshold set for the identification of an ERE majorly depends on the climatology of the region. In order to identify the thresholds for the identification of cloudbursts in this study, a quantitative determination has been performed and plots have been generated for the study region which is included in Appendix III. It can be seen that the rainfall intensities usually increase gradually with associated percentile but there is a sudden jump in values above 99.90 percentile. As discussed in section 2.3, previous researchers usually associated 90th, 94th, 95th, 99th and above percentiles as thresholds (Bookhagen 2010, Goswami *et al*. 2010, Krishnamurthy *et al*. 2009, Malik *et al*. 2011, May 2004). Since, it is not possible to check all the thresholds in this study, therefore, in order to check the appropriate threshold as the ERE index, we restrict this study with the analysis of three

percentiles 98th, 99th and 99.99th exclusively. The following flow chart elaborates the steps taken for the analysis of extremes:

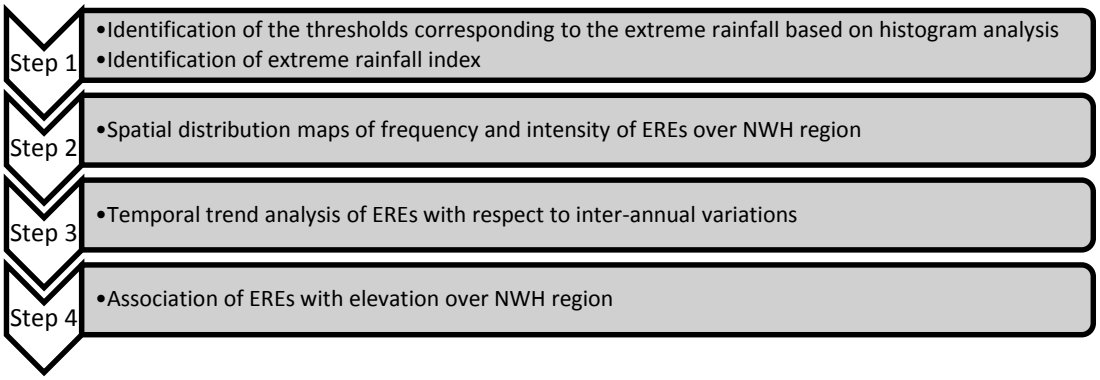

Figure 4.2: Steps for the analysis of EREs

In order to determine whether there is a change in the extreme events, trend analysis has been performed with the help of the following statistical measures:

i) Student's t test for hypothesis testing

Student's t-test has been performed on the dataset with null hypothesis that data are a random sample from a normal distribution with mean zero and unknown variance against the alternative hypothesis that mean is not equal to zero. The single sample t-test produces result in the form of acceptation or rejection of null hypothesis.

H_0 : The mean of the sample is equal to zero, symbolically

$$H_0: \mathrm{X} = \mu = 0$$

H_1 : The sample mean is different than zero,

$$H_1 : \mathrm{X} = \mu \neq 0$$

ii) Correlation Analysis

In order to analyze the co-variation of two or more variables, correlation analysis has been performed and regression equation has been calculated to quantify the strength of their relation. The equation of Karl Pearson's has been discussed in section 4.4.3. In our study, correlation analysis has been found out between frequency and intensity of EREs with elevation.

4.4.5 Comparative analysis of Kedarnath and Leh case studies

In the recent times, Leh and Kedarnath were two mammoth disasters related to cloudburst events which caused massive number of casualties and huge economic losses. In this study, a comparative analysis between Kedarnath and Leh cloudburst events examining various atmospheric parameters in addition to precipitation has also been carried out for the sake of outlining similarities and differences between both the events. The analysis has been performed using the atmospheric parameters derived from MODIS dataset listed in section 4.1.3, as well as the TRMM and IMD datasets for precipitation analysis.

The coarser resolution MODIS dataset is performed only on one pixel pointing at the respective locations. However, the precipitation analysis has been performed on two grid points of TRMM data for Leh and Kedarnath which includes the nearby surrounding areas also. The monthly rainfall has been examined for the months of June 2013 and August 2010 for Kedarnath and Leh respectively. Further rainfall of past 16 years has also been analysed for the month of June for Kedarnath and August for Leh region respectively. The spatial plots of diurnally propagating rain bands elucidates the movements and intensity of rain bands.

5. RESULTS AND DISCUSSION

This chapter discusses the results obtained from the research work. The major objectives of this research were to validate the satellite rainfall data with ground based measurement and further extraction of spatiotemporal trend over the NWH region. The chapter begins with the section 5.1 which deals with the validation of TRMM data with IMD data in order to achieve the first major objective of this research. The subsequent two sections 5.2 and 5.3 deal with the spatial and temporal analysis of the ERE over the region in order to seek out the answer for the second major objective. The next segment i.e. section 5.4 seeks out the answer to the research question pertaining to any association of topography with frequency and intensity of EREs. The last section 5.5 deals with the third major objective i.e. the comparative analysis between Kedarnath and Leh events. Other than the first section, only TRMM data has been used for the analysis of precipitation in the rest of the sections.

5.1 Validation of TRMM data with IMD data

The TRMM data has been validated with the ground based IMD data using the methodology discussed in section 4.4.3. First, the general performance of TRMM is addressed followed by a closer examination of few cloudburst events and spatial distribution of mean seasonal precipitation.

5.1.1. Correlation analysis

The Pearson's linear correlation coefficient was calculated between the mean seasonal rainfall derived by IMD and TRMM 3B42 v7 data sets using scatterplot over the NWH. With the sample size 494, each dot represents a pixel in NWH having the mean seasonal rainfall during monsoon months for 16 years (1998-2013). The graph shows a positive correlation of 0.88 (r^2=0.77) indicating direct relation between both the variables. The slope of regression line was found to be positive and correlation was found to be significant even at 1% ($p \sim 0$) significance level. Zulkafli *et al.* (2014), who conducted their study over six climate regions also agrees that TRMM 3B42 version 7 data better correlates with rain gauge data than previous version.

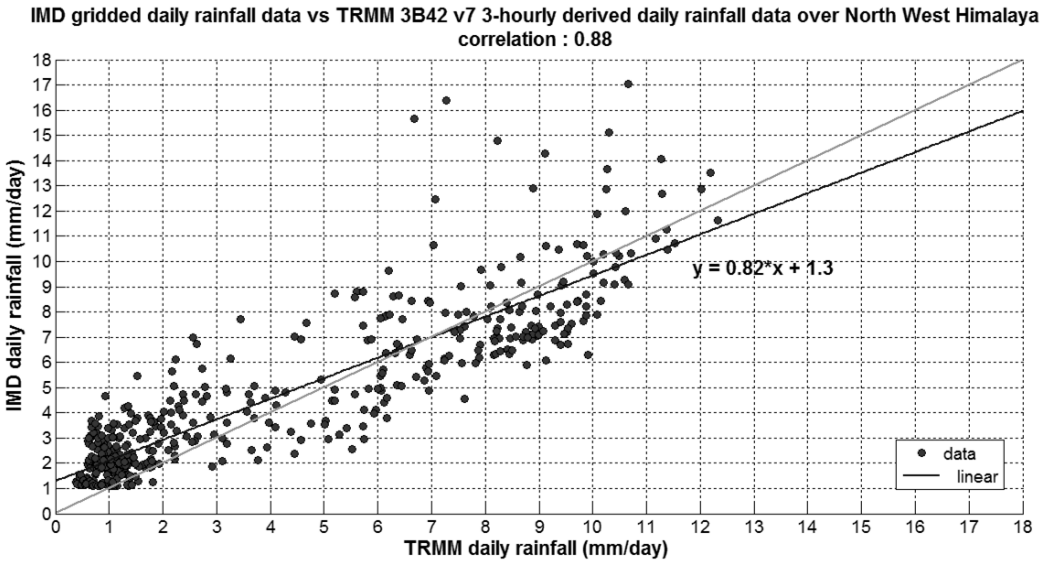

Figure 5.1: Correlation between IMD derived average daily rainfall data (represented on y-axis) and TRMM derived average daily rainfall (shown on x-axis) data for each pixel in NWH region. The light colored line is 1:1 line. The dark color line shows the linear fitting of the data.

Javanmard *et al*. (2010) also found good correlation of 0.77 between TRMM 3B42 v6 and rain gauge data over high mountainous region of Iran. Xie *et al.* (2007) found a correlation of ~0.7 between Chinese rain gauges and TRMM 3B42 v6 data. Fang *et al*. 2013 also found correlation of 0.6 – 0.8 between downscaled TRMM 3B42 v7 data and ground based measurements over mountainous region of Xiao river basin. Present analysis reveals that there is a strong correlation between IMD data and TRMM data over the NWH region which is in concurrence with the previous studies. The positive slope and intercept of the regression line (y = 0.82x + 1.3) indicates that in general TRMM underestimates low mean seasonal rainfall and overestimates high mean seasonal rainfall.

5.1.2. Analysis of few case studies

Further, in order to evaluate the performance of TRMM in estimating extreme rainfall events, a list has been prepared. It includes a few major cloudburst events occurred in the NWH region in the past 16 years and the rainfall amounts as captured by TRMM and IMD are compared. The locations of these cloudburst events has been shown in the figure 5.4 (a). The IMD and TRMM rainfall amounts are calculated on the surrounding regions which includes more than one pixel. As for most of the cloudbursts, the documentation of exact date and time was not available, rainfall amounts represent accumulated rainfall for multi-dates (days) as mentioned in the table 5.1.

Table 5.1: List of cloudburst events occurred in the NWH region taken for the analysis with specific location dates, TRMM and IMD rainfall amounts and its bias

Year	Days	Location (Place, District)	State	original latitude	original longitude	IMD rainfall amount (mm)	TRMM rainfall amount (mm)	Bias (IMD – TRMM)
2013	June 15-17	Kedarnath, Rudraprayag	UT	30.734	79.066	691.3	812.2	-120.9
2010	Aug 5-6	Leh, Ladakh	J&K	34.125	77.577	42.2	257.2	-215
2011	July19-20	Rohtang La, Manali	HP	32.239	77.188	65.5	80	-14.5
2011	June 8-9	Doda, Jammu	J&K	33.046	75.62	60.3	161.2	-100.9
2010	Aug11-13	Khonmoh, Srinagar	J&K	34.056	74.947	81.5	100.5	-19
2010	Sep15-20	Katarmal, Almora	UT	29.848	79.322	941	690	251
2012	Sep12-15	Ukhimath, Rudraprayag	UT	30.515	79.096	26.2	464.5	-438.3
2013	Aug 1	Kapkot, Bageshwar	UT	29.938	79.902	154.8	591.5	-436.7
2012	Aug2-8	Bhatwari, Uttarkashi	UT	30.818	78.616	754.9	499.3	255.6
2009	Aug6-7	Munsyari, Pithoragarh	UT	30.072	80.237	156.2	302.2	-146

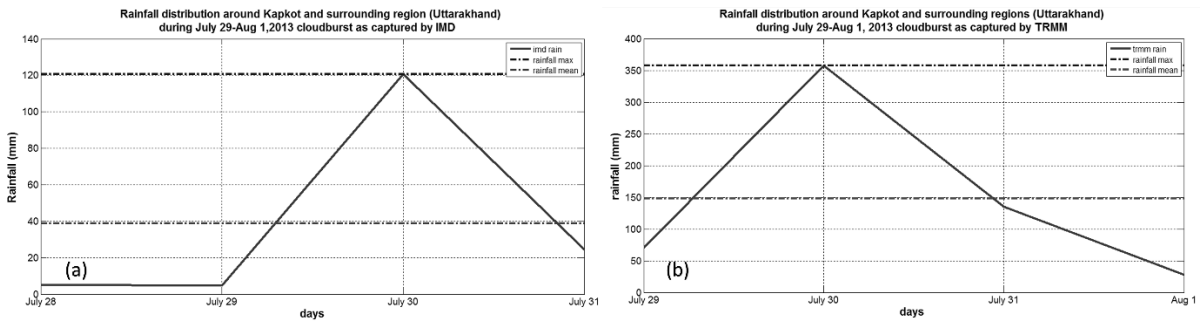

Figure 5.2: Rainfall distribution around Kapkot and nearby regions during cloudburst event on July 29-August 1, 2013 as captured by (a) IMD data (b) TRMM data

Out of the 10 events, TRMM recorded higher rainfall intensity in 8 of the events as compared to IMD data. The rainfall graphs of Leh and Kedarnath events will be discussed under the section 5.6 where an extensive study has been done using other meteorological parameters also for these two events. The rainfall distribution plot for Kapkot cloudburst event has been shown in the figure 5.2. The rainfall plots for the rest of the events can be found in the Appendix II. 80% of the times, a huge discrepancy (>100 mm) between the satellite and ground based rainfall has been observed during an extreme event. This may be due to problems associated with precipitation measurements on either or both sides. As the number of gauges is very limited in the Himalaya region, most of the gauges are still installed in the valley floors (Andermann *et al*. 2011, Palazzi *et al*. 2013 and references therein) which may miss the signatures of the cloudburst due to its highly localized nature. In other cases, the rain gauge itself is subjected to destruction due to the hazard.

These findings of overestimation by TRMM data for extreme rainfall events seems to be in line with results obtained by previous studies. TRMM 3B42 v7 data overestimated the rainfall amount for Beijing ERE in July 2012 as studied by Huang *et al*. (2013) in their detailed analysis. Jamandre and Narisma (2013) through their analysis of extremes over Philippines concluded that TRMM 3B42 v6 captures the extremes well however it overestimates the rainfall amount during extreme weather event. Li *et al*. (2013) suggest that TRMM 3B42 v6 overestimates the heavy intensity rainfall, but is better at estimating the frequency of occurrence of precipitation than rain gauge. All these studies were conducted over mountainous region with >1000 m elevation. However, though TRMM overestimates the rainfall intensity of cloudburst events, yet it captures the occurrence of most of the events which is in agreement with Jamandre and Narisma (2013) and Li *et al*. (2013).

5.1.3. Comparison of spatial pattern of mean seasonal precipitation

The spatial distribution of mean seasonal (JJAS) precipitation has been derived from IMD and TRMM data sets as shown in figure 5.2. It has been observed that the spatial distribution of rainfall is well captured by TRMM data. However, the satellite overestimates and underestimates data at some regions. In order to find out the locations of over and under estimations by satellite, rainfall bias has been calculated by subtracting the rain estimates captured by TRMM from the IMD dataset and is generated as the map shown in figure 5.4 (b).

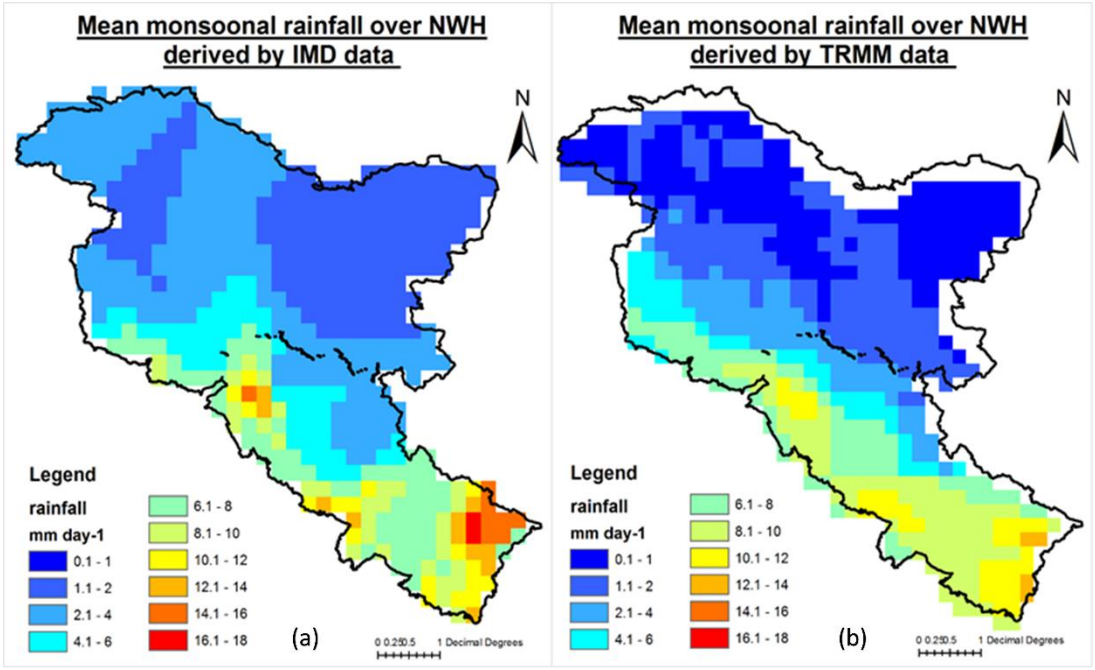

Figure 5.3: Mean seasonal precipitation as derived by (a) IMD data (left panel) and (b) TRMM data (right panel) respectively over NWH using 16 years (1998 – 2013) rainfall data

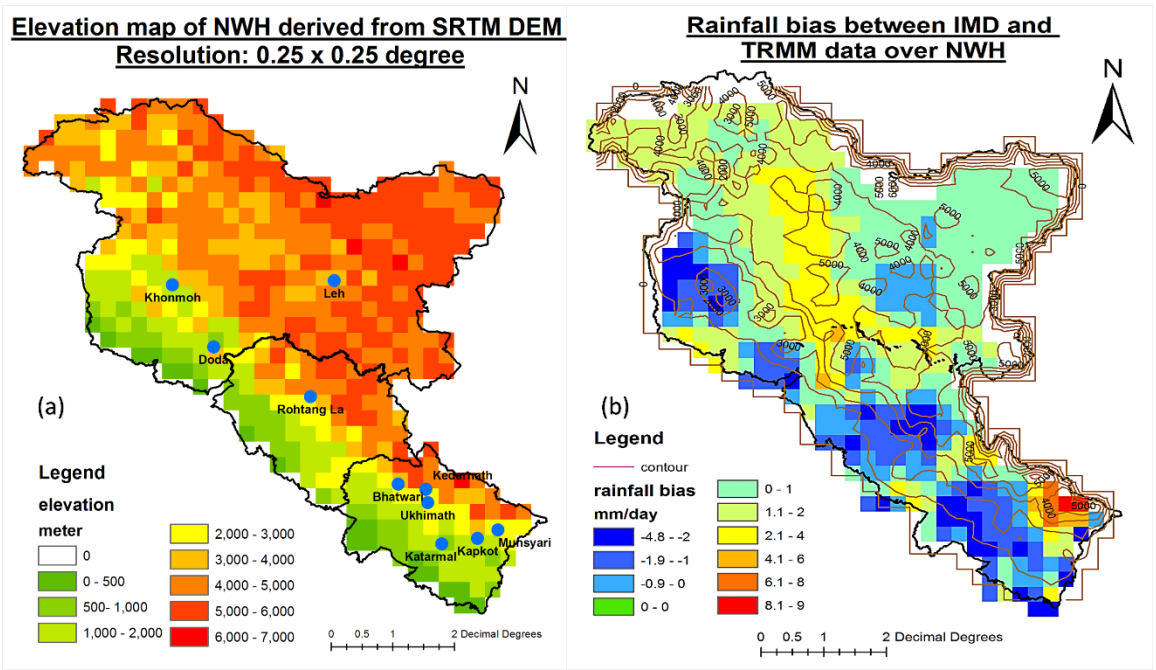

Figure 5.4: (a) Elevation map of NWH generated using resampled SRTM DEM (b) Rainfall bias map generated for NWH region with contours depicting elevation ranges in meter (0 contour line is present on the borders due to absence of raster data outside NWH region)

The rainfall bias map was then overlaid with the Elevation map generated by SRTM DEM which was resampled at 0.25° resolution to match the resolution of precipitation data is shown in figure 5.4. TRMM data overestimates the rainfall having minimum bias as -4.85 mm day^{-1} over areas with <3000 m elevation whereas it underestimates the rainfall having maximum bias as 8.52 mm day^{-1} at regions with elevation >3000 m which is in agreement with the study conducted by Andermann *et al.* (2011). The average bias

was found to be 0.56 mm day^{-1}. It has been reported that several factors including topography, relief, retrieval algorithms and type of season determine the performance of the satellite precipitation measurements (Li *et al*. 2013, Andermann *et al*. 2011, Nasrollahi 2015). Sapiano and Arkin (2009) mentioned that satellite precipitation products (including TRMM) give better estimations in warm season. As satellite precipitation estimation relies heavily on cloud-top temperature, it can easily underestimate rainfall in orographic regions where warm-rain processes are responsible for orographic precipitation (Li *et al*. 2013 and references therein, Nasrollahi 2015 and references therein, Zulkafli *et al*. 2014 and references therein). It has also been observed that TRMM has relative low bias as compared to other satellite estimates, although no measurement technique is free from bias (Smith *et al*. 2006). Here, TRMM is not only overestimating rainfall at region with up to 3000 m elevation but also in rain shadow regions. Hence, the behaviour of satellite data over mountainous regions remains an open question for further research.
Therefore, on the basis of above analysis it has been observed that TRMM data normally follows IMD data, hence, can be used for the study of extreme rainfall events.

5.2 Identification of Extreme Rainfall Index

5.2.1 Histogram analysis

The probability distribution functions such as precipitation rate distribution or histogram provide an effective way to understand the precipitation characteristics. The figure 5.5 depicts the precipitation rate distribution for daily rainfall during monsoon season over the NWH region. It has been constructed by organizing the daily rainfall of past 16 years into a frequency distribution. This frequency distribution has been decided on the basis of classes or bins with 50 mm day^{-1} width. It conveys how likely a particular rainfall amount event occurs. Figure 5.5 portrays skewed right distribution i.e. the frequency of rainfall events decreases gradually with increasing rainfall intensity. As expected, the high number of rainfall events usually have less than 25 mm day^{-1} rain rate. Moreover, very heavy precipitation incidents are usually rare in the region.

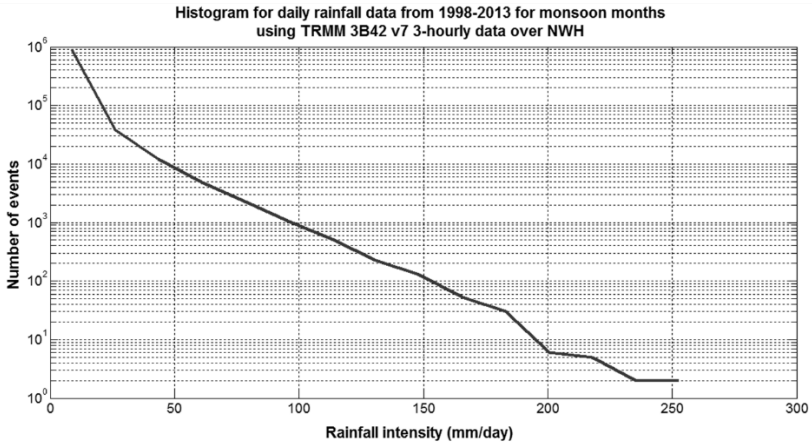

Figure 5.5: Histogram of TRMM derived daily rainfall for monsoon season of 1998-2013 for NWH region. The number of events is shown in natural log scale.

As the extreme events are considered as rarest of the rare, to identify the threshold for the extreme rainfall index, three percentile thresholds 98th, 99th & 99.99th will be examined in the study. The rainfall intensities for 98th, 99th and 99.99th thresholds have been calculated for the whole of NWH and also separately for each state. The table 5.2 shows the rainfall intensities obtained for different thresholds over study regions.

Table 5.2 - Rainfall intensities associated with 98th, 99th & 99.99th percentiles for NWH and the states of Uttarakhand, Himachal Pradesh and Jammu & Kashmir

Region	98th percentile (mm/day)	99th percentile (mm/day)	99.99th percentile (mm/day)
NWH	36.57	50.72	157.09
Uttarakhand	59	74.7	179.9
HP	46.15	61.26	160.79
J&K	17.51	26.49	123.38

The table 5.2 highlights the huge variations in rainfall intensities associated with different regions within the NWH. As the region experiencing highest mean monsoonal rainfall, Uttarakhand also has highest rainfall intensities associated with all three percentiles. This is due to the reason that the strength of monsoon decreases south to north along the mountain barrier and east to west along the path of the travel of the monsoon (Basistha *et al.* 2007 and references therein). Therefore, monsoon intensity decreases as it moves from Uttarakhand towards HP and J&K contributing to low rainfall intensities associated with the percentile thresholds.

98th and 99th percentiles may be considered as extreme and very extreme rainfall events, whereas the 99.99th percentile may correspond to cloudburst events. The percentile plots over NWH region shown in figure (b) of Appendix III depicts that 98th and 99th percentile plots somehow follow each other but the 99.99th percentile plot does not seem to share any similarity with the other two. The precipitation analysis conducted for Leh and Kedarnath events shows that precipitation intensity for both the events is above 99.99th percentile. Therefore, the 99.99th percentile can be defined as the extreme rainfall index corresponding to the rarest of the rare precipitation events or cloudburst events.

5.2.2 Spatial distribution of extreme rainfall events over the Northwest Himalaya

The 1-day maximum precipitation amount has been calculated for each grid of the NWH region, for the past 16 years and for each day of 122-days long monsoon season (as shown in figure 5.6).

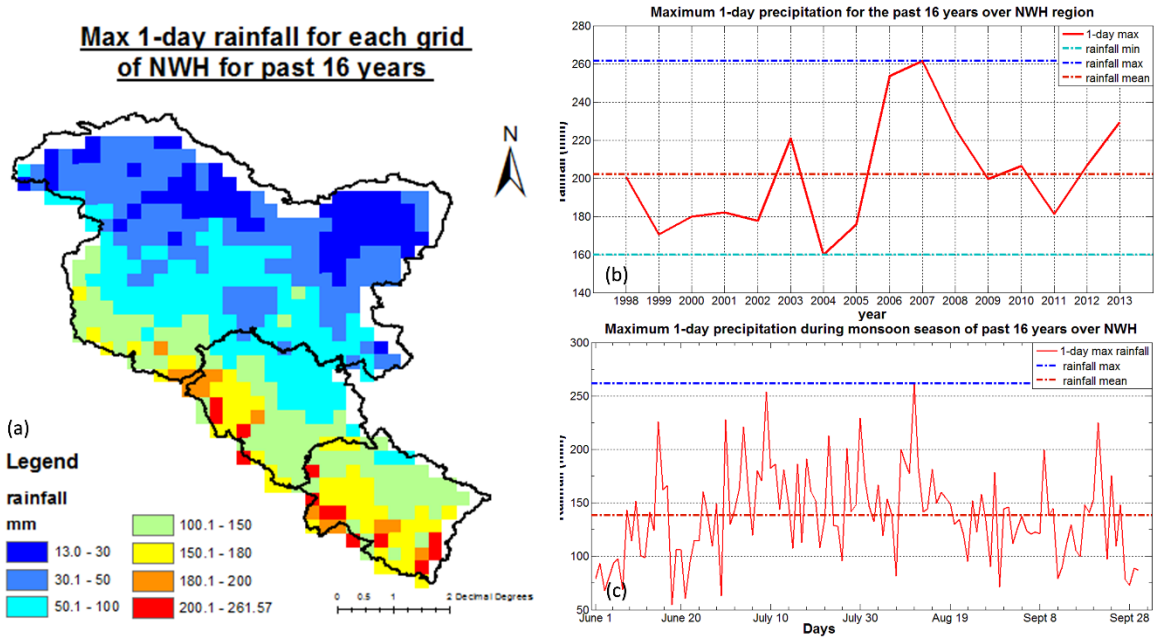

Figure 5.6: Maximum 1-day precipitation event (a) spatial distribution for each grid of NWH (b) year-wise plot for the past 16 years i.e. 1998-2013 (c) day-wise plot during monsoon season of past 16 years

The spatial distribution of max 1-day rainfall event mimics the mean monsoonal rainfall distribution (as shown in figure 5.3). The highest precipitation events (>=200) were captured at below 2000 m elevation. The highest 1-day precipitation amount is found as 261.57 mm day^{-1}. It is also noteworthy that in the year 2007, the mean monsoonal rain was around average, but it experienced highest 1-day precipitation of the past 16 years (as seen in figure 5.6 (b)). The maximum 1-day precipitation has also been captured throughout the monsoon season, even before the official onset and near the withdrawal phase as seen in figure 5.6 (c). It gives an insight that a very intense precipitation can happen any time during the monsoon period.

Further, the areal averaged maps have been generated for the NWH region depicting the spatial distribution of the frequency of EREs with rainfall intensities associated with three scenarios: 1) number of EREs having intensity >=98th percentile and <99th percentile (2) number of EREs having intensity >=99th percentile and <99.99th percentile (3) number of EREs >=99.99th percentile. From the figure 5.7 it can be derived that the spatial distribution of frequency of EREs closely follows the spatial patterns of mean seasonal rainfall (refer to Appendix IV) and 1-day maximum rainfall. The frequency of EREs decreases with the increasing elevation and becomes rather rare on high peaks. Out of the three states, larger areas of Uttarakhand are prone to EREs comparatively. We also observe that mountains of Uttarakhand region receive higher frequency of EREs than of Himachal Pradesh and J&K. This observation may again be attributed to the stronger strength of the monsoon in Uttarakhand than the other two states as discussed in section 5.2.1.

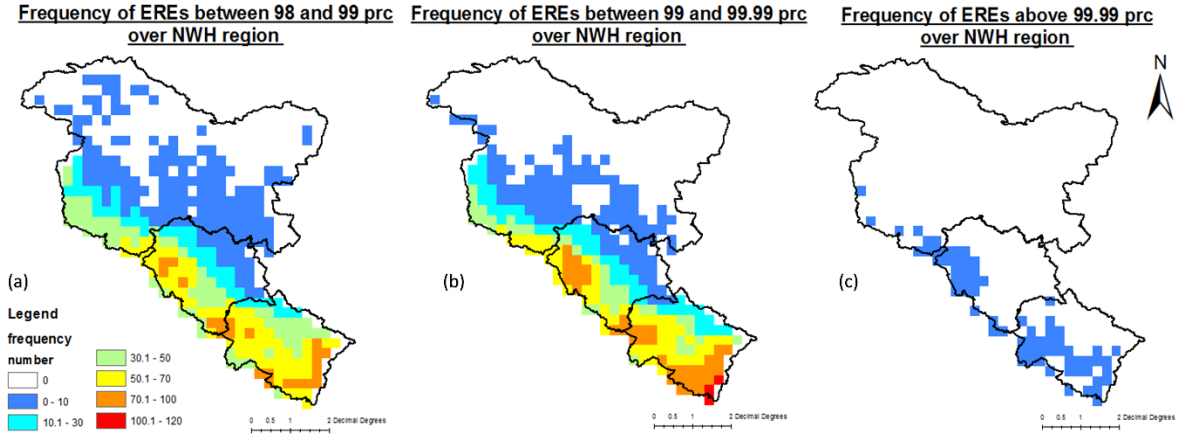

Figure 5.7: Spatial distribution of frequency of EREs over NWH for (a) frequency of EREs with intensity >=98th & <99th percentile (b) same as (a) but for >=99th & <99.99th percentile (c) same as (a) but for >=99.99th percentile

It can be observed that frequency of events decreases over all the regions for increasing percentile thresholds. The frequency of EREs exceeding 99.99th percentile is not more than 5 for any pixel with district of Champawat (Uttarakhand) receiving maximum (5 EREs) number of EREs exceeding 99.99th percentile. In HP and J&K, the EREs above 99.99th percentile threshold are strongly restricted to regions with <3000 m elevation. The leeward side of J&K receives very little rainfall, consequently the frequency of EREs is also negligible. Jamandre and Narisma (2013) studied TRMM version 6 over Philippines and indicated that sometimes TRMM tends to overestimate the frequency of events exceeding 100 mm rainfall and also falsely counts the frequency over regions which have never experienced an ERE. Li *et al.* (2013) also reported overestimation of frequency of intense rainfall events by TRMM. However, these observations are also highly location-specific. The analysis performed using few cloudburst studies in the

section 5.1.2 has already showed that TRMM version 7 is good at estimating the frequency of occurrence of EREs. It is important to note that an ERE does not necessarily mean a disaster. The prospect of an ERE turning into a disaster depends on various geographical and anthropogenic factors.

The rainfall is a local process featuring huge spatial variability. Thus, the rainfall intensities associated with 98th, 99th & 99.99th percentile for each pixel have been analyzed for the NWH region as shown in the figure 5.8.

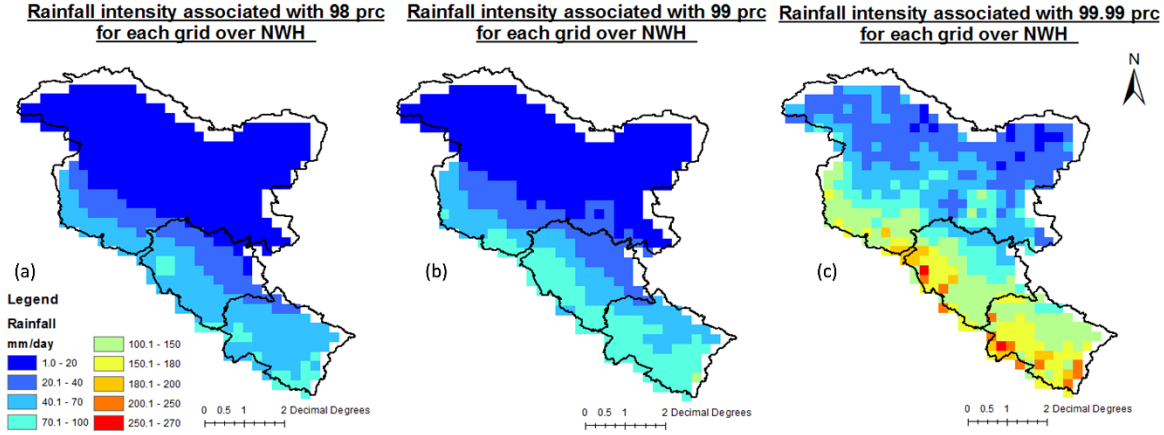

Figure 5.8: Rainfall intensities for each pixel/grid of NWH for (a) 98th percentile (b) 99th percentile (c) 99.99th percentiles during monsoon season of the period 1998 – 2013

Not surprisingly, the lower elevated regions show higher rainfall intensities of EREs. The distribution of pixel wise rainfall intensities also seem to follow the elevation distribution order especially the distribution of rainfall intensities associated with 98th and 99th percentile. However, there are some regions which experience very heavy rainfall out of the blue while the some other regions receiving steady rainfall rate almost never experience an ERE. This clearly highlights the extremely inconsistent nature of rainfall even within the specified region. Moreover, even the high elevated regions which experience little rainfall are not entirely excluded from experiencing EREs. Even the regions like Kargil and Ladakh which experience as low average rainfall as 1.8 mm day^{-1} and 1.3 mm day^{-1}, have experienced EREs with rainfall intensities 120 mm day^{-1} and 101 mm day^{-1} respectively. It highlights the unpredictable and sporadic nature of EREs.

5.3 Trend analysis of extreme rainfall events over the Northwest Himalaya

Although only 16 years of precipitation data might be inadequate to comment on the trend of EREs, nevertheless an attempt has been made which might elucidate the use of satellite precipitation data for the study of EREs in future. Keeping the prime research objective of performing trend analysis of EREs over the region in mind, the temporal trend of inter-annual frequency of EREs has been analyzed. In the figure 5.9, number of events have been calculated and plotted for each year for the three scenarios – (1) number of EREs having intensity >=98th percentile and <99th percentile (2) number of EREs having intensity >=99th percentile and <99.99th percentile (3) number of EREs >=99.99th percentile. To find whether the slope of regression line is significantly different than zero, student's t-test was performed. The null hypothesis states that the slope is zero i.e. there's no trend present and the alternate hypothesis states that the slope is not equal to zero i.e. some trend is present.

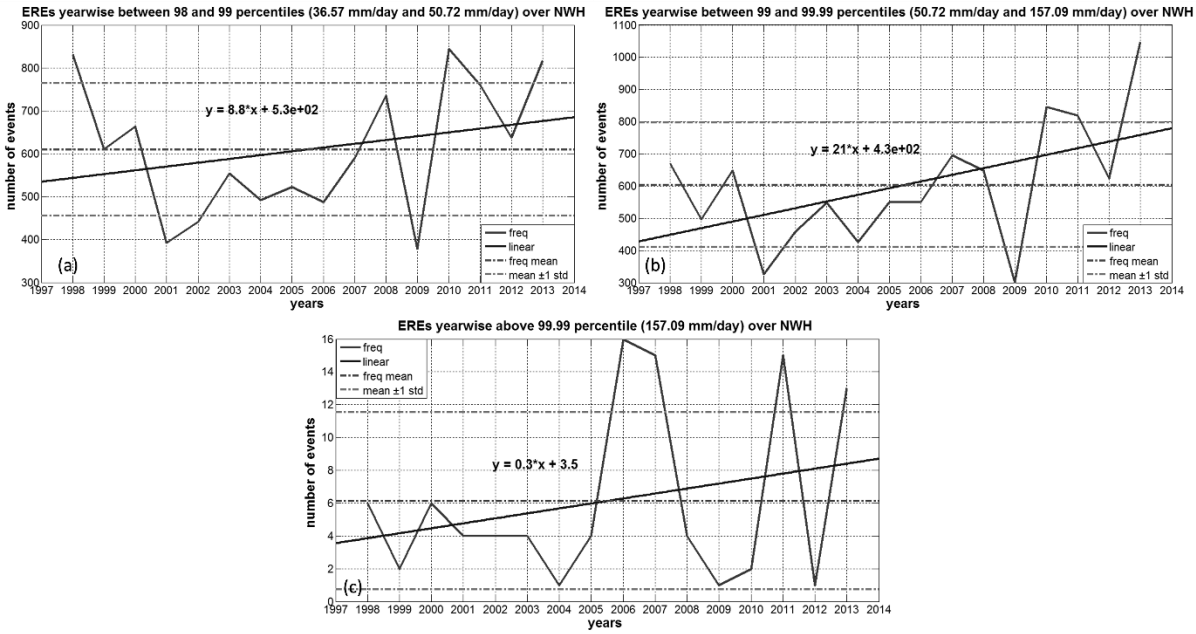

Figure 5.9: Inter-annual variation of frequency of EREs over NWH for (a) frequency of EREs with intensity >=98th & <99th percentile (b) same as (a) but for >=99th & <99.99th percentile (c) same as (a) but for >=99.99th percentile; x-axis represents the years and y-axis shows the total number of EREs over NWH

The test results for inter-annual plots for all three scenarios indicate that the slope is significant even at 1% significance level (p-value is close to 0) i.e. an increasing trend of EREs is evident for all three scenarios which is in agreement with Sen Roy (2009) who also reported a strong positive trend of extremely heavy rainfall events during monsoon season over both foothills and high elevated areas of northwestern Himalaya using station level precipitation data for the period 1980 – 2002. It is illustrated in the figure 5.9 that mostly the oscillations are well within the ±1 standard deviation limits of mean suggesting that there may be regional factors responsible for such trend rather than external factors. The limited number of EREs exceeding 99.99th percentile threshold points out at the oddity of events. It is interesting to note that the highest number of events exceeding 99.99th percentile was registered in the year 2006, when the average seasonal rainfall was below mean; whereas the year 2010 recorded highest mean seasonal precipitation but experienced very less EREs exceeding 99.99th percentile. Analysis shows that frequency of EREs exceeding 98th and 99th percentiles correlated well with mean monsoonal rainfall with correlation coefficient ~0.9 but no correlation was found between mean seasonal rainfall and frequency of EREs exceeding 99.99th percentile. Thus, it can be said with conviction that frequency of very heavy rainfall events has no correlation with mean seasonal rainfall. The similar trend analysis has been done for the states also (plots not included). The results show positive trend for all three scenarios for all three states indicating that frequency of EREs is increasing even at state level.

5.4 Association of elevation with extreme rainfall events

In the interest of establishing any relation of elevation with frequency and intensity of EREs, it would be reasonable to first understand the association of mean seasonal rainfall with elevation for the region. The correlation analysis has been executed between mean seasonal rainfall and elevation which shows strong negative correlation between both factors with negative slope of the regression line. The correlation coefficients for NWH, Uttarakhand, HP and J&K are found to be -0.82, -0.67, -0.86 and -0.73 respectively. The figures have been included in the appendix V. These results imply that mean monsoonal

rainfall decreases with increasing elevation as seen in figure 5.2 also and conforms to the previous studies by Shreshta *et al.* 2012 and Singh & Kumar 1997.

In pursuance of relation between elevation and EREs, similar approach has been adopted. The figure 5.10 depicts the 3-dimensional representation of the extremely variable topography of NWH region. The figure presents a good illustration of steadily increasing elevation from southwest to northeast direction of NWH region. The NWH region is characterized by a one-step topography (Bookhagen 2010).

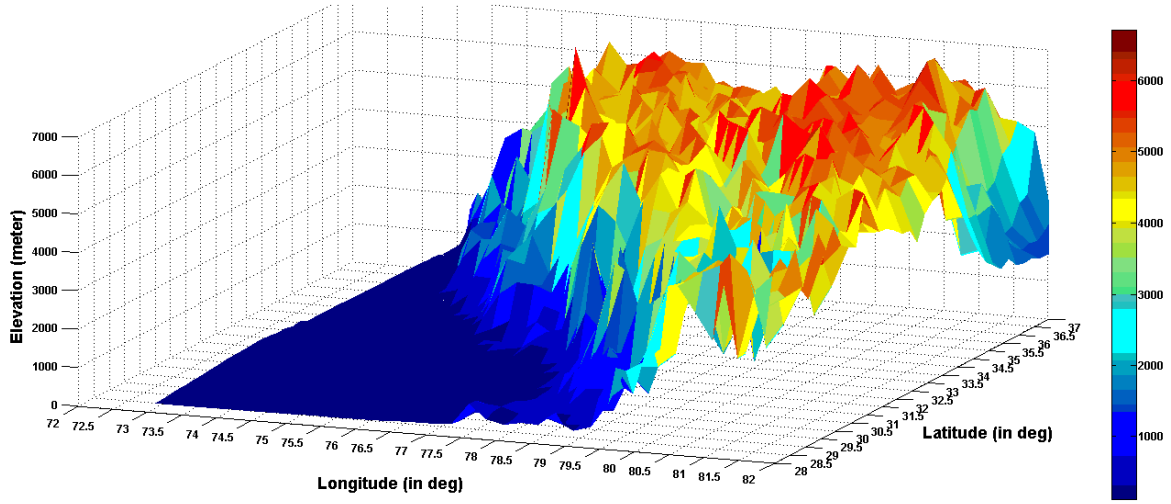

Figure 5.10: 3D representation of elevation of NWH region as derived from SRTM DEM resampled at 0.25° resolution; x-axis represents latitude , y-axis represents longitude and z-axis represents elevation in meter above mean sea level; The direction of view is from southeast to northwest. The colour bar indicates elevation in meter.

Though various factors related to topography affect rainfall such as elevation, slope, aspect, relief, geometry etc. (Anders *et al.* 2006, Houze Jr. 2012), here, an effort has been made exclusively to outline any relation of elevation with EREs. Firstly, the correlation analysis has been performed between the frequency of EREs for 98th, 99th & 99.99th percentile thresholds and the elevation of the region. The figure 5.11 shows the results obtained. The results show strong negative correlation between elevation and the frequency of EREs exceeding 98th & 99th percentile thresholds. The slope of the regression line is found to be negative for both cases, indicating decrease in frequency with increasing elevation with highest number of events at <500 m elevation.

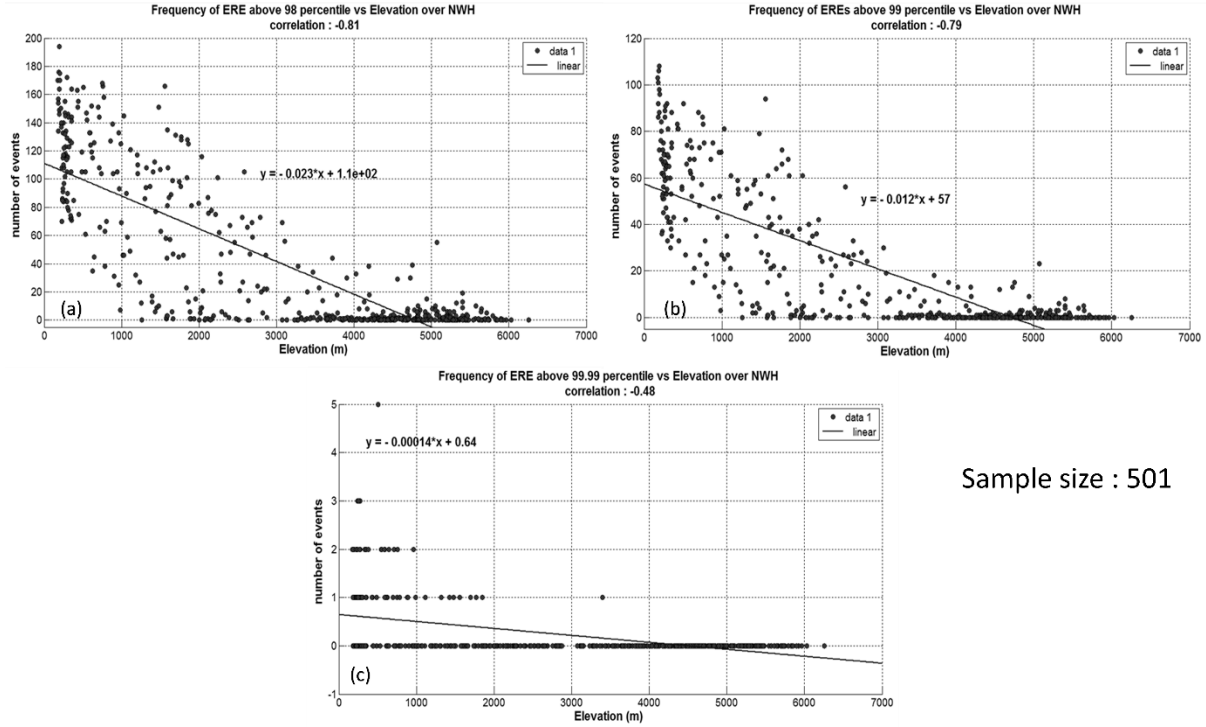

Figure 5.11: Correlation analysis between elevation and frequency of EREs for (a) >=98th percentile (b) >=99th percentile (c) >=99.99th percentile over NWH region for the past 16 years from 1998 to 2013.

However, weak negative correlation has been found between EREs exceeding 99.99th percentile and elevation. Moreover, the events exceeding 99.99 percentile are practically absent over regions having elevation above 4000 m. The majority of EREs occur up to 3000 m altitude which supports the spatial distribution of EREs observed in the section 5.2.2 (refer figure 5.7).

Further step includes studying the correlation of the rainfall intensities associated with 98th, 99th & 99.99th percentiles with the elevation of the region for each pixel. The findings has been shown in the figure 5.12. The analysis shows a strong negative correlation between rainfall intensities associated with 98th, 99th & 99.99th percentiles and elevation suggesting inverse relation. The negative slope of regression line points out, as the elevation increases the strength of EREs decreases which further is in agreement with the results obtained in section 5.2.2 (refer figure 5.8). However, for all the percentiles, strong negative relation can be found for the rainfall intensity ranging from 20-80 mm day^{-1} and up to 3000 m elevation. The low rainfall intensity corresponding to <20 mm day^{-1} and the elevation greater than 3000 m do not correlate well.

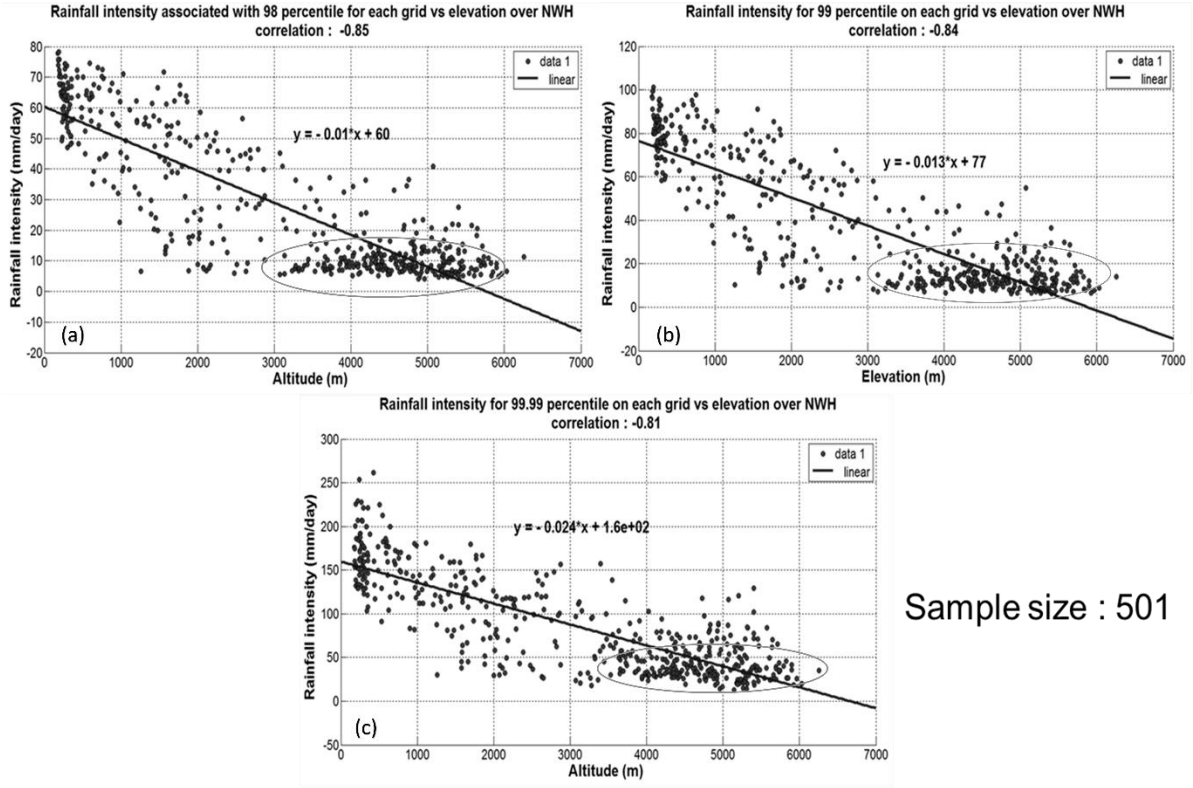

Figure 5.12: Correlation analysis between elevation and rainfall intensities associated with (a) 98th percentile (b) 99th percentile (c) 99.99th percentile for each pixel of NWH region for the period 1998 – 2013

The inverse relation derived from figure 5.11 and 5.12 supports that not only mean seasonal rainfall decreases with elevation but the frequency & intensity of EREs too.

Next step includes analysis of frequency of EREs with respect to different elevation ranges (bins of 500 and 1000 m) over NWH which is shown in the figure 5.13.

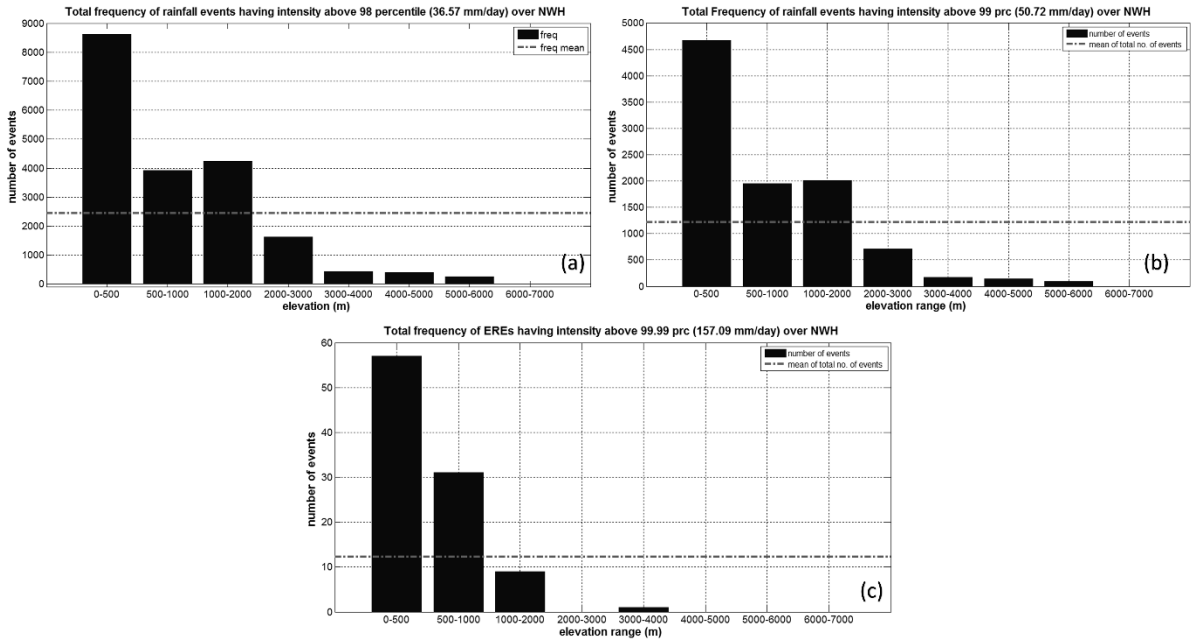

Figure 5.13: Plots depicting frequency of EREs for different elevation ranges over NWH region for (a) 98th percentile (b) 99th percentile (c) 99.99th percentile for the period 1998-2013

The x-axis represents the elevation ranges with the difference of 500 m and y-axis represents the frequency of EREs. The plains and foothills (up to 500 m) receive the highest number of EREs and the frequency decreases as we proceed towards higher elevations. Though the decrease is not gradual as the ranges between 1000 – 2000 m elevations receive almost similar number of EREs exceeding 98th and 99th percentile thresholds as 500 – 1000 m ranges. However there is a steady decrease in the frequency of EREs exceeding 99.99th percentile threshold with elevation. The frequency of EREs exceeding 99.99th percentile threshold is almost absent for regions above 3000 m elevation as seen from the figure 5.13.
Similar analysis was carried out for the three states also, and high frequency of EREs up to 2000 m elevation exceeding 98th and 99th percentiles has been observed for Uttarakhand and J&K. However, the frequency of EREs above 99.99th percentile is highest at foothills i.e. up to 500 m elevation for Uttarakhand and J&K. For HP, the highest frequency has been observed at 500-1000 m elevation for all three percentiles.

5.5 Comparative analysis of Leh and Kedarnath events

5.5.1 Precipitation analysis

Leh town of the Ladakh district experienced calamitous flash floods due to extreme rainfall during August 4-6, 2010. It is acknowledged as the worst calamity ever in the region as it took roughly 255 lives with hundreds missing (Thayyen *et al.* 2013 and references therein). The Leh cloudburst event was a unique phenomenon which sparked interest in scientific community due to its highly localized nature which was unable to be captured by the nearest meteorological station that recorded only 12.8 mm/day rainfall (Thayyen *et al.* 2013).

Kedarnath, a small town in Uttarakhand state experienced an extremely unusual multi-date ERE during June 15-17, 2013 resulting in devastating floods the state ever experience. The disaster was termed as 'Himalayan tsunami' due to its sheer enormity causing an unparalleled loss of human lives and infrastructure. It is also known as the worst natural disaster of India since 2004 tsunami. It had resulted in thousands of fatalities and missing people and the complete wipe-out of entire towns and several villages.

The few similarities and differences between the static factors can be underlined here. Leh and Kedarnath both are situated at around 3500 m elevation from mean sea level. However, Leh is situated at the leeward side of the Himalaya range whereas Kedarnath is situated at the windward side. As Leh falls into the rain shadow region it receives mean monsoonal precipitation of 1.21 mm day^{-1} whereas Kedarnath experiences heavy monsoon rainfall with mean monsoonal precipitation of 6.97 mm day^{-1}.

In this study, an analysis of precipitation and cloud properties has been executed for a better understanding of both the EREs. Moreover, the analysis has been presented in a comparative fashion allowing a distinct overview of the underlying similarities and contrasts between both the events. In the figure 5.14, the spatial and temporal aspect of precipitation received during the Kedarnath and Leh events are presented here simultaneously.

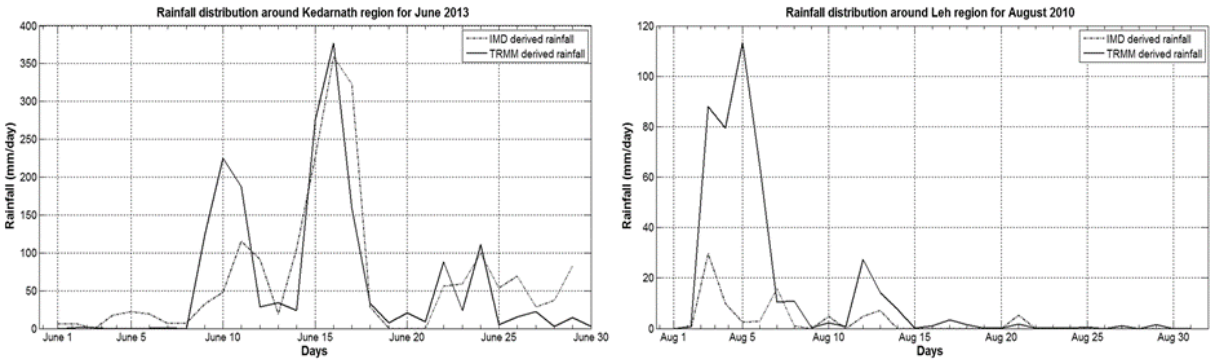

Figure 5.14: Rainfall distribution using TRMM and IMD data for (a) Kedarnath region for the month of June, 2013 (b) Leh region for the month of August 2010

The figure 5.14 shows the rainfall amount registered during the month of June 2013 and month of August 2010 over Kedarnath and Leh area respectively by both TRMM and IMD. For the Kedarnath disaster, both IMD and TRMM have captured almost similar rainfall quantities exceeding 350 mm/day on June 16, 2013. However, for Leh event IMD clearly has failed to register the extraordinary amount of rainfall occurred during August 2010 but TRMM captured above 100 mm/day rainfall for August 5, 2010.
Further, the rainfall amount captured around Kedarnath region for June month and around Leh region for August month during the last 16 years has been shown in the figure 5.15.

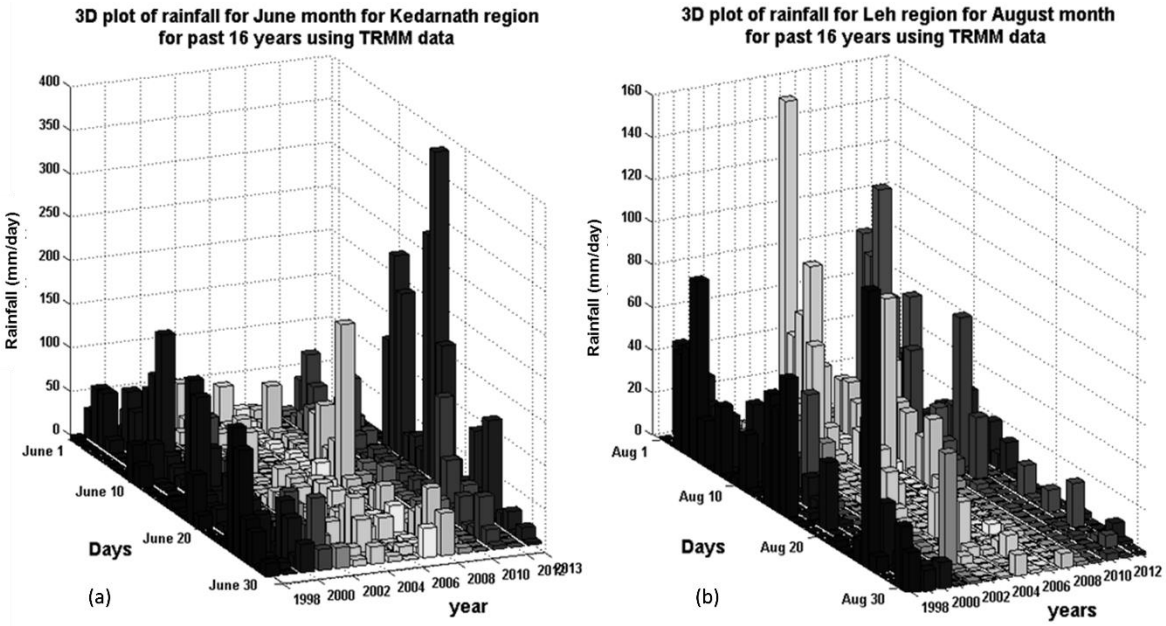

Figure 5.15: 3D rainfall plots for (a) Kedarnath region for June month of past 16 years (b) Leh region for August month of past 16 years respectively; x-axis represents the year, y-axis represents the number of days (June for Kedarnath and August for Leh) and z-axis for rainfall amount

It is quite apparent that rainfall registered during June 15-17 in the year 2013 was a never-seen-before event at least in the past 16 years in Kedarnath region. During August 2006 floods (Thayyen *et al.* 2013), the highest rainfall event was registered by TRMM in Leh region on August 1, 2006. The floods were also an unusual event, however, we will be focusing only on August 2010 cloudburst event.
In the next step, the spatial analysis of rainfall and the propagation of rain bands with 3-hour interval during Kedarnath and Leh events have been observed sequentially.

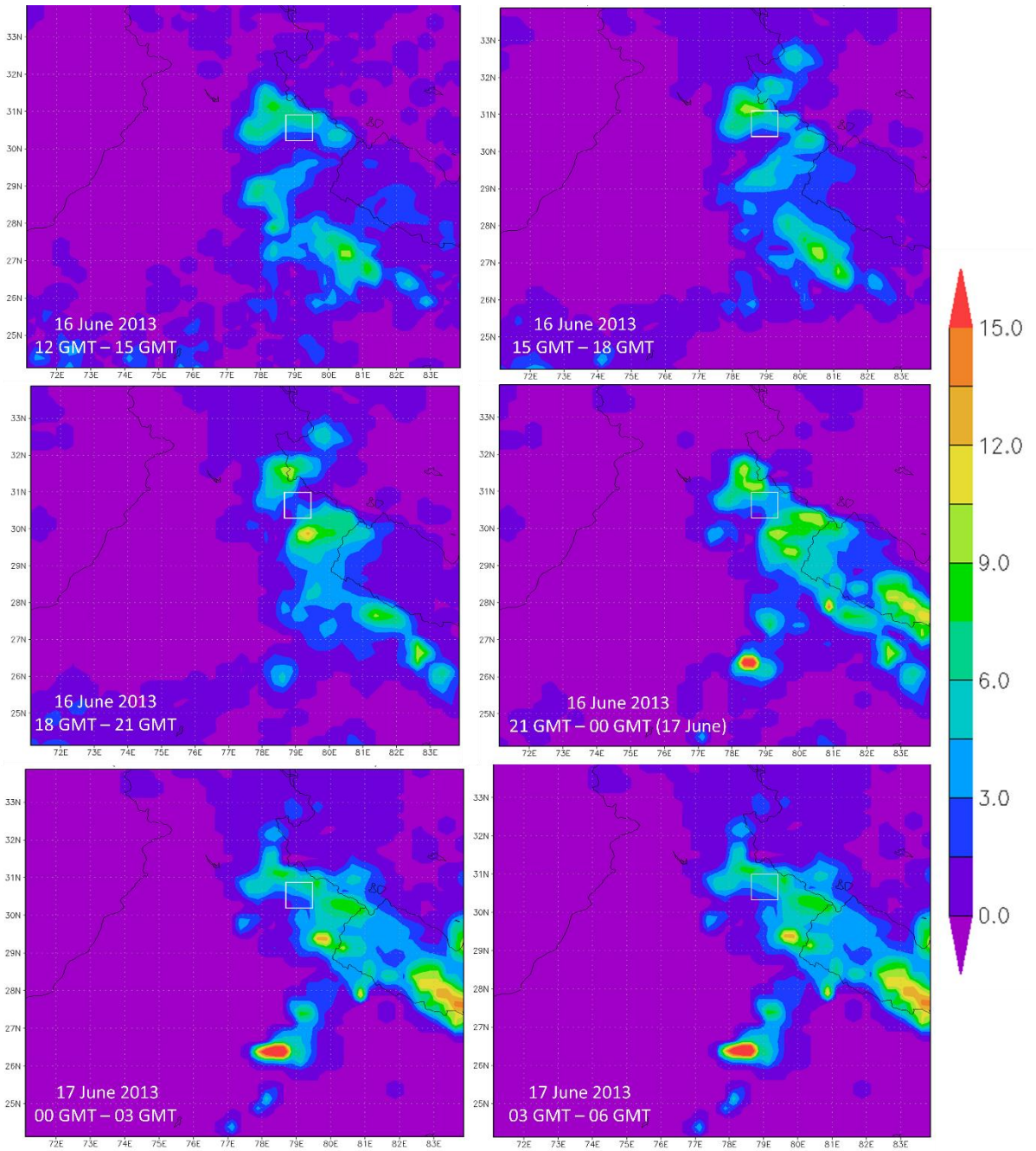

Figure 5.16: Position and intensity of rain bands prior and after the Kedarnath cloudburst event. The maps are plotted for 3-hour temporal resolution. The colour bar indicates the rainfall intensity in mm/h. The location of Kedarnath town is shown as white rectangle in the maps.

Two different rain bands, one coming from the southwest direction seem to have originated in Bay of Bengal and the other originated in Arabian Sea coming from northwest direction. Both the rain bands merge into one rain band over Rajasthan (please refer to appendix VI for all the plots) and propagate towards Kedarnath region where it becomes highly intense. However, this event was not very localized as the rain bands spread all over the Uttarakhand and HP states giving rise to heavy rainfall throughout the region for several days. The deluge continued even after the Kedarnath cloudburst which was reported at June 16-17, 2013 midnight to early morning (Rautela 2013). Therefore, only the plots for June 16 midnight

to June 17 early morning duration are included in figure 5.16. The rain bands further departed from Uttarakhand Mountains and proceeded towards Nepal region.

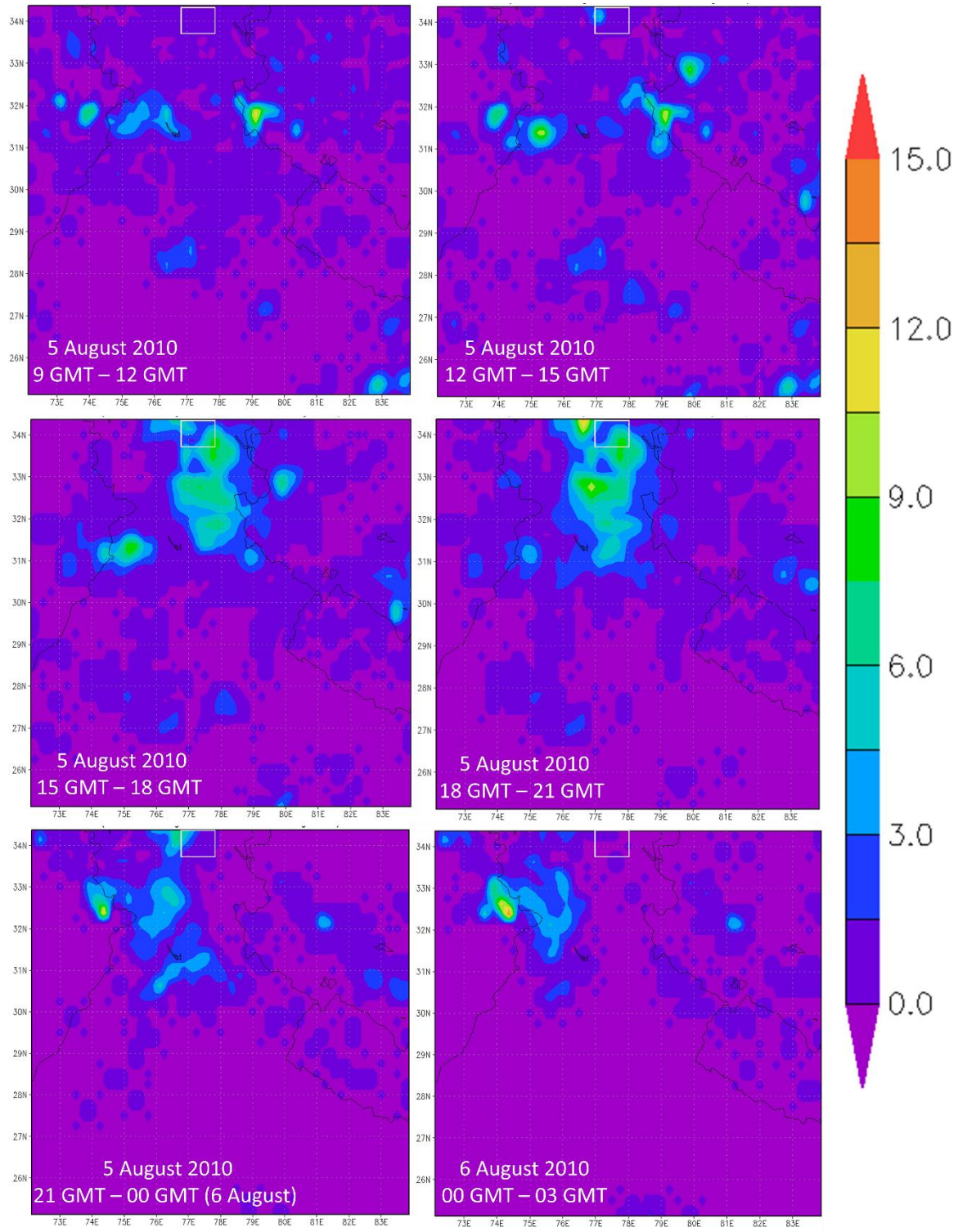

Figure 5.17: Position and intensity of rain bands prior and after the Leh cloudburst event. The maps are plotted for 3-hour temporal resolution. The colour bar indicates the rainfall intensity in mm/h. The location of Leh town is shown as white rectangle in the maps.

From the figure 5.17 it can be observed that on August 5, 2010 around 09 – 12 GMT (1430 – 1730 IST) no rainfall was seen over Leh area. However, two rain bands coming from different directions, one from

northwest and the other from southeast direction travelling with velocity approximately 1°/h merge over Leh region at around 15 – 18 GMT (2030-2330 IST) and caused heavy rainfall. After 21 GMT (0230 IST) there is no rainfall recorded over Leh region and the rain bands further moved towards Pakistan region. Unlike Kedarnath event when surrounding areas also received heavy rainfall, this was a localized event and was focused over Leh region.

Further, the atmospheric parameters as mentioned in section 4.4.5 have been compared for both of the events as obtained from Aqua and Terra sensors of MODIS satellite. The results are discussed here:

5.5.2 Cloud Top Temperature (CTT)

The Infrared based rainfall measurements from space are indirect measurements that takes cloud top temperature into account and estimate the precipitation using empirical relations (Nasrollahi 2015, Liu & references therein 2003, Rosenfeld 2007). In general, colder CTT corresponds to higher rainfall rates for convective clouds (Liu 2003). Low temperature indicates high cloud tops with greater thickness and larger probability of rain (Barrett and Martin 1981, Punay and Perez 2014). Hanna *et al*. (2008) classified precipitation type with cloud-top brightness temperature. They identified –45°C for light rain, –47°C for moderate rain, and –50°C CTT peaks for heavy rain along with –5° to 0°C CTT peaks corresponding to warm rain process. The daily variation of the CTT over the Kedarnath and Leh region during the ERE events as illustrated in the figure 5.18 respectively.

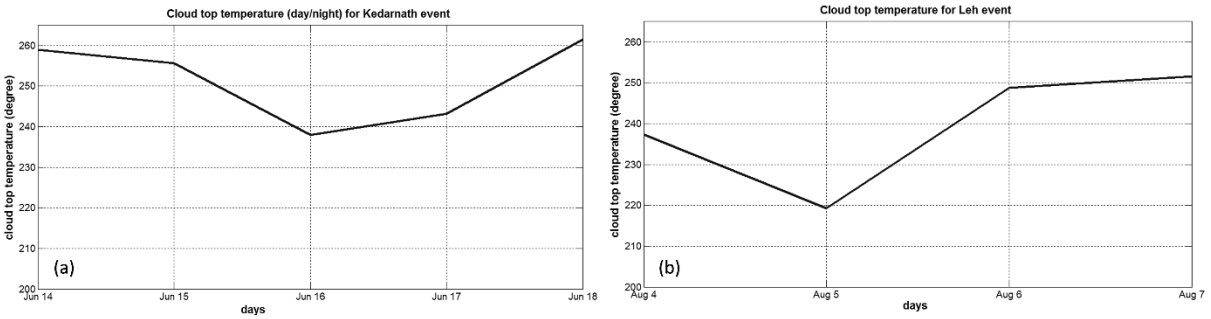

Figure 5.18: cloud top temperature profile for (a) Kedarnath event (b) Leh event

The CTT for Kedarnath disaster varies from -35.22°C to -11.59°C whereas for Leh event it is measured as low as -53.92°C and up to -21.53°C. The clouds were cooler during Leh event than Kedarnath event suggesting presence of thicker clouds capable of heavier rainfall at Leh. However, the rainfall measurements during Kedarnath event were much higher than Leh.

5.5.3 Cloud Top Pressure (CTP)

The cloud top pressure determines the cloud top height from the mean sea level. As the atmospheric pressure decreases with increasing height, the low cloud top pressure indicates the huge vertical height of the cloud capable of producing heavy rainfall.

Furthermore, the cloud top pressure for both the events have been compared in the following figure 5.19:

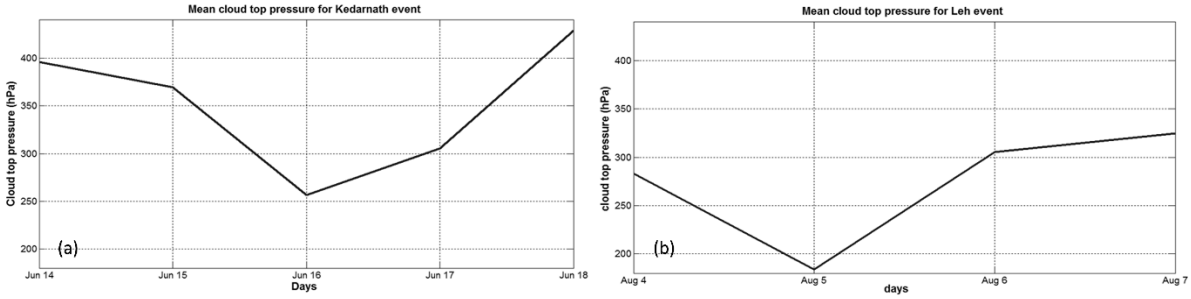

Figure 5.19: cloud top pressure profile for (a) Kedarnath event (left panel) (b) Leh event (right panel)

It can be seen that lowest CTP of Leh event was registered as 183.60 hPa suggesting cloud height of up to approx. 12295 m above msl on August 5, 2010 and during Kedarnath event the minimum was registered as 256.8 hPa indicating cloud height of up to approx. 10184 m above msl. Both the results indicate at the presence of vertically developed cumulonimbus clouds generated either due to thermal convection or frontal lifting as towers capable of producing powerful thunderstorms and very heavy rainfall. As the time progresses, the CTP increases and cloud height decreases to 6600 m for Kedarnath and 8600 m for Leh event.

5.5.4 Cloud Fraction

The cloud fraction determines the percentage of a pixel which was covered with clouds with values ranging from 0 to 1.

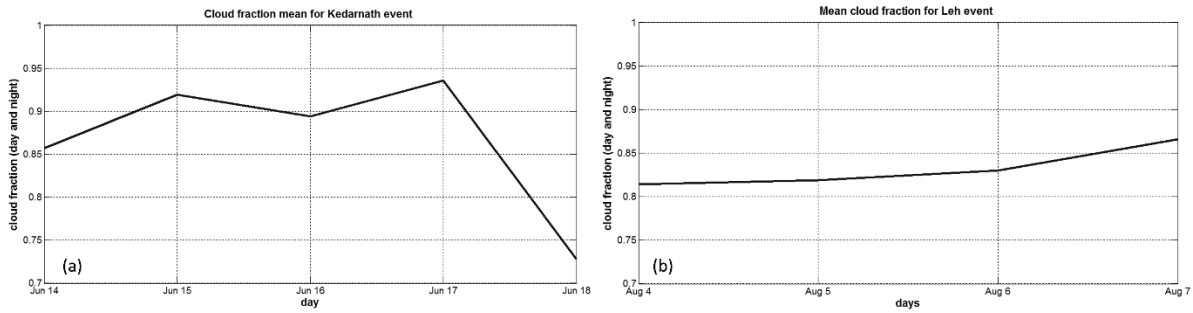

Figure 5.20: cloud fraction profile for (a) Kedarnath event (left panel) (b) Leh event (right panel)

The cloud fraction profile during both the events indicates there was more than 80% cloud cover. However, combining the results of CTT and CTP, it can be concluded that other than June 16, 2013 and August 5, 2010, these clouds were less cold and low in height incapable of generating sudden vehement deluge.

5.5.5 Cloud Optical Depth (COD)

In broad sense, cloud optical depth measure the opacity of the atmosphere and is dimensionless. The value can range from 0 to 100 with 100 meaning completely opaque atmosphere (Punay and Perez 2014 and references therein). Clouds with higher depth correspond to greater cloud thickness which indicates higher probability of precipitation with greater intensity (Barrette & Martin 1981).

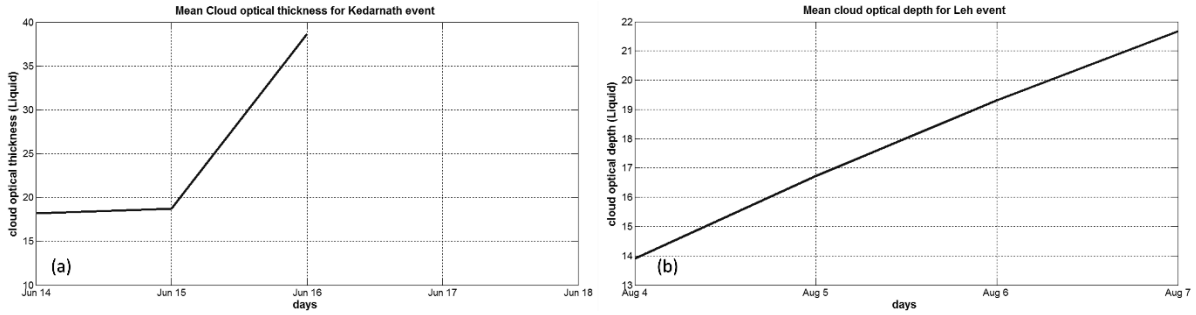

Figure 5.21: Cloud optical depth during (a) Kedarnath event (left panel) (b) Leh event (right panel)

The optical depth of the clouds of Kedarnath event is higher than that of Leh event. The higher value relates to the high vertical cloud structure. The relation between the cloud parameters CTP and COD has been derived by International Satellite Cloud Climatology Project (ISCCP) as a table which can be found in appendix VII. According to the table, the cloud type during Kedarnath and Leh events has been observed. The high COD (between 35 - 40) and low pressure of 256.8 hPa correspond to deep convection which indicates the possibility of occurrence of cloudburst. However, for Leh event the CTP was 183.60 hPa but the COD has been registered between 16 - 17. This points at the cloud type of cirrostratus which cannot be possible as cirrostratus clouds do not cause cloudburst. Hence, it can be concluded that the MODIS sensor did poor estimation of cloud optical depth during the Leh event.

6. CONCLUSION AND RECOMMENDATIONS

Motivated by the recent occurrences of disastrous extreme rainfall events in the Northwest Himalaya region and the increasing concerns about their behaviour in future, this research has been conducted to study the spatiotemporal variations of the extreme rainfall phenomenon over the Northwest Himalaya region during the monsoon season. This study utilized TRMM 3B42 version 7 satellite precipitation data available from 1998 to 2013. A strong positive correlation of 0.88 was found between TRMM 3B42 v7 data and ground based measurements supporting the use of satellite precipitation data for the study over Northwest Himalaya. However, TRMM data underestimates mean seasonal rainfall over regions with elevation >3000 m and overestimates over regions with <3000 m elevation. The range of rainfall bias lies between -4.85 mm day^{-1} to 8.52 mm day^{-1} with average bias of 0.52 mm day^{-1}. Further, TRMM overestimates the rainfall amount for extreme rainfall events but is good at capturing the frequency of extreme events. However, the tendency of satellite for over- or underestimation of rainfall highlights the need for further research for the modification of rainfall retrieval algorithm over mountainous regions.

The study identified the extreme rainfall index after the analysis of extreme rainfall events using three percentile thresholds 98^{th}, 99^{th} & 99.99^{th}. It is suggested that 98^{th} and 99^{th} percentile thresholds may be considered as extreme and very extreme events whereas 99.99^{th} percentile threshold may correspond to the cloudburst events. During the two major extreme rainfall events *viz.* Leh and Kedarnath events rainfall exceeding 99.99^{th} percentile was experienced over the respective regions. Further, the spatial and temporal analysis of the extreme rainfall events over the Northwest Himalaya region indicates decrease in frequency and intensity of extreme rainfall events with increasing elevation. The high frequency of extreme rainfall events is majorly restricted to regions with <3000 m elevation. The frequency of extreme rainfall events exceeding 99.99^{th} percentile is not more than 5 for any pixel of the region with district of Champawat in Uttarakhand experiencing highest 5 cloudburst events. Moreover, the frequency and intensity of extreme rainfall events is greater for Uttarakhand as compared to the other two states of Himachal Pradesh and Jammu & Kashmir. Further trend analysis has been performed using the statistically robust test. A statistically significant (significant at 1% significance level) increasing trend has been found for the frequency of extreme events. A positive trend has also been discovered for the cloudburst events over the region. The analysis done at state level also indicates an increasing trend for all three states.

Furthermore, the relation between extreme rainfall events and elevation was analysed for the study region. A strong negative correlation (~0.8) was found between the frequency of EREs exceeding 98^{th} and 99^{th} percentiles and elevation but poor negative correlation (~0.48) was found between the frequency of cloudbursts and elevation over the NWH. The strong negative correlation of -0.85, -0.84 and -0.81 was found between elevation and rainfall intensity associated with 98^{th}, 99^{th} & 99.99^{th} percentiles respectively. However, this strong negative correlation was restricted to rainfall intensity up to 20 – 80 mm day^{-1} and elevation up to 3000 m. The low rainfall intensity corresponding to <20 mm day^{-1} and the elevation greater than 3000 m do not correlate well. Therefore, nothing conclusive can be commented for these ranges. It has also been observed that plains and foothills of Northwest Himalaya with elevation up to 500 meter receive the higher number of extreme rainfall events, nonetheless for Himachal Pradesh the highest frequency of extremes was observed at 500 – 1000 m elevation range and for Uttarakhand at 1000 – 2000 m. It is suggested to carry out a detailed analysis to understand the precipitation processes as a function of topography over the two mountainous states *viz.* Himachal Pradesh and Uttarakhand of the Northwest Himalaya.

In addition to this, a few conclusions can be outlined through the comparative analysis of meteorological and atmospheric parameters during Leh and Kedarnath events. Though both were catastrophic disasters, however, Leh was a more spatially and temporally focused event. During Kedarnath event, the rain bands can be seen to have spread over a large area indicating it as a more extensive phenomenon at both spatial and temporal scales. The cloud parameters CTT, CTP, cloud fraction and COD also provide a unique view of studying the cloudburst events and may prove useful in future for the now casting of the cloudburst events.

Recommendations

The following recommendations are suggested after completing this research:

- Although satellite provides an excellent mean for studying precipitation over inaccessible regions, however, TRMM satellite tends to over and underestimate rainfall over orographic regions. Therefore, further modifications in rainfall retrieval algorithm are suggested for mountainous regions. The reasons for such behavior of the satellite also remain an open question for further research.

- The relation between elevation and frequency of extreme rainfall events should be studied separately state wise for Uttarakhand, Himachal Pradesh and Jammu & Kashmir. This study has been limited to examining the relation between elevation and rainfall exclusively, however, other topographical factors like slope, aspect and geometry of the region may also be the reason for such dissimilar results which need to be studied elaborately.

- Though robust statistical tests have been used for the trend analysis, however small sample size is a limitation. The usage of long term dataset is recommended for the future work. Further, regional level analysis may help in better prediction of trend of extreme rainfall events.

- The results of this research are meant as an assistance in the field of disaster management. Policy-makers are expected to follow the research outcomes and plan infrastructure accordingly in cloudburst prone regions. The spatial distribution study of the extreme rainfall events may be helpful in the systematic documentation of events.

LIST OF REFERENCES

Alpert P (1986) Mesoscale Indexing of the Orographic Precipitation over High Mountains. Journal of Climate and Applied Meteorology. Volume 25: 532-545.

Anders A M, Roe G H, Hallet B, Montgomery D R, Finnegan N J and Putkonen J (2006). Spatial patterns of precipitation and topography in the Himalaya. Geological Society of America. Special Paper 398. DOI:10.1130/2006.2398 (03).

Andermann C, Bonnet S and Gloaguen R. (2011) Evaluation of precipitation data sets along the Himalayan front. Geochemistry Geophysics Geosystems, 12, Q07023. DOI: 10.1029/2011GC003513.

Ashok K, Guan Z and Yamagata T (2001) Impact of the Indian Ocean Dipole on the relationship between the Indian Monsoon Rainfall and ENSO. Geophysical Research Letters, Vol. 28. No. 23, Pages 4499-4502. http://dx.doi.org/10.1029/2001GL013294.

Attri S D and Tyagi A (2010) Climate Profile of India. Contribution to the Indian Network of Climate Change Assessment (National Communication-II) Ministry of Environment and Forests. India Meteorological Department, Ministry of Earth Sciences. Met Monograph No. Environment Meteorology-01/2010.

Barrette E C and Martin D W (1981) The Use of Satellite Data in Rainfall Monitoring. Academic Press Inc. (London) Ltd, ISBN: 0-12-079680-5.

Barros A P, Kim G, Williams E and Nesbitt S W (2004) Probing orographic controls in the Himalayas during the monsoon using satellite imagery. Natural Hazards and Earth System Sciences (2004) 4: 29–51. DOI: 10.5194/nhess-4-29-2004.

Barry R G (2008) Mountain Weather and Climate Third Edition. Cambridge University Press. Online ISBN: 9780511754753. http://dx.doi.org/10.1017/CBO9780511754753.003.

Basistha A, Arya D S and Goel N K (2007) Spatial Distribution of Rainfall in Indian Himalayas – A Case Study of Uttarakhand Region. Water Resource Management 22, 1325–1346. DOI: 10.1007/s11269-007-9228-2.

Basistha A, Arya D S and Goel N K (2009) Analysis of Historical Changes in Rainfall in the Indian Himalayas. International Journal of Climatology 29: 555–572. DOI: 10.1002/joc.1706.

Bhan, S C, Devrani A K and Sinha V (2015) An analysis of monthly rainfall and the meteorological conditions associated with cloudburst over the dry region of Leh (Ladakh), India. Mausam, 66, 1 (January 2015), 107-122.

Bookhagen B (2010) Appearance of extreme monsoonal rainfall events and their impact on erosion in the Himalaya. Geomatics, Natural Hazards and Risk 1(1):37-50. DOI: 10.1080/19475701003625737, March 2010.

Bookhagen B and Burbank D W (2006) Topography, relief, and TRMM-derived rainfall variations along the Himalaya. Geophysical. Research Letters vol. 33, L08405. DOI: 10.1029/2006GL026037.

Bookhagen, B and Burbank D W (2010) Toward a Complete Himalayan Hydrological Budget: Spatiotemporal Distribution of Snowmelt and Rainfall and Their Impact on River Discharge. Journal of Geophysical Research Vol. 115, F03019. DOI: 10.1029/2009JF001426.

Bookhagen B, and Strecker M R (2008) Orographic barriers, High-resolution TRMM rainfall, and Relief Variations along the Eastern Andes. Geophysical Research Letters Vol. 35, L06403. DOI: 10.1029/2007GL032011.

CGIAR CSI SRTM 90m DEM Digital Elevation Database. http://srtm.csi.cgiar.org/ . Accessed on: December 13, 2014.

Chen Y, Ebert E E, Walsh K J E and Davidson N E (2013) Evaluation of TRMM 3B42 Precipitation Estimates of Tropical Cyclone Rainfall using PACRAIN Data. Journal of Geophysical Research: Atmospheres, Vol. 118, DOI: 10.1002/jgrd.50250.

Chopra R (2014) Uttarakhand: Development and Ecological Sustainability. Oxfam India, June 2014.

Chow F K, Wekker S F D and Snyder B J (eds.) (2013) Mountain Weather Research and Forecasting, Recent Progress and Current Challenges. Springer Atmospheric Sciences. ISBN 978-94-007-4098-3. DOI: 10.1007/978-94-007-4098-3.

Das P K (2002) Monsoons. National Book Trust. ISBN: 9788123711232.

Das P K (2013) 'The Himalayan Tsunami' - Cloudburst, Flash Flood & Death Toll: A Geographical Postmortem. IOSR Journal Of Environmental Science, Toxicology And Food Technology (IOSR-JESTFT) e-ISSN: 2319-2402. p- ISSN: 2319-2399. Volume 7, Issue 2 (Nov. - Dec. 2013), PP 33-45.

Das S, Ashrit R and Moncrieff M W (2006) Simulation of a Himalayan Cloudburst Event. Journal of Earth System Science 115(3):299–313. DOI: 10.1007/BF02702044.

Dhar O N and Rakhecha P R (1980) The Effect of Elevation on Monsoon Rainfall Distribution in the Central Himalayas. Monsoon Dynamics. J Lighthill and R P Pearce, Eds, Cambridge University Press, 253-260.

Dinku T, Chidzambwa S, Ceccato P, Connor S J and Ropelewski C F (2008) Validation of High-Resolution Satellite Rainfall Products over Complex Terrain. International Journal of Remote Sensing 29, 4097–4110. DOI: 10.1080/01431160701772526.

Dobhal D P, Gupta A K, Mehta M and Khandelwal D D (2013) Kedarnath disaster: facts and plausible causes. Current Science 105(2):171-174.

Ebtehaj M and Foufoula-Georgiou E (2010) Orographic Signature on Multiscale Statistics of Extreme Rainfall: A Storm-Scale Study. Journal of Geophysical Research: Atmospheres 115, 1–14. DOI: 10.1029/2010JD014093.

Fang J, Du J, Xu W, Shi P, Li M and Ming X (2013) Spatial Downscaling of TRMM Precipitation Data Based on the Orographical Effect and Meteorological Conditions in a Mountainous Area. Advances in Water Resources 61 (2013) 42–50. http://dx.doi.org/10.1016/j.advwatres.2013.08.011.

Francis P A and Gadgil S (2006) Intense Rainfall Events over the West Coast of India. Meteorology and Atmospheric Physics 94:27–42. DOI: 10.1007/s00703-005-0167-2.

Planning Commission Himachal Pradesh. Geographical Features of Himachal Pradesh.

Ghosh S, Das D, Kao S and Ganguly A R (2011) Lack of uniform trends but increasing spatial variability in observed Indian rainfall extremes. Nature Climate Change, Vol. 2, February 2012. DOI: 10.1038/nclimate1327.

Giovanni-3 Online Users Manual: 8 MOVAS Giovanni. Giovanni-3 Online Users Manual: 8 MOVAS Giovanni. http://disc.sci.gsfc.nasa.gov/giovanni/additional/users-manual/G3_manual_Chapter_8_MOVAS.shtml. Accessed on: January 02, 2015.

Goswami B B, Mukhopadhyay P, Mahanta R and Goswami B N (2010) Multiscale interaction with topography and extreme rainfall events in the northeast Indian region. Journal of Geophysical Research: Atmospheres Volume 115, Issue D12, 27 June 2010. DOI: 10.1029/2009JD012275.

Goswami B N, Venugopal V, Sengupta D, Madhusoodanan M S and Xavier P K (2006) Increasing Trend of Extreme Rain Events Over India in a Warming Environment. Sciencemag.org 10.1126/science.1132027

Goswami P and Ramesh K V (2007) Extreme Rainfall Events: Vulnerability Analysis for Disaster Management and Observation System Design. Current Science 94(8):1037-1044.

Guhathakurta P and Rajeevan M (2006) Trends in the rainfall pattern over India. National Climate Centre Research Report No: 2/2006.

Guhathakurta P, Sreejith O and Menon P (2011) Impact of climate change on extreme rainfall events and flood risk in India. Journal of Earth System Science 120, No. 3, June 2011, pp. 359–373.

Hanna J W, Schultz D M and Irving A R (2008) Cloud-top temperatures for precipitating winter clouds. Journal of Applied Meteorology and Climatology 47(1):351–359.

Hennessey K J, Gregory J M and Mitchell J F B (1997) Changes in daily precipitation under enhanced greenhouse conditions, Climate Dynamics, 13, 667–680.

Himachal Pradesh Development Report. Himachal Pradesh: A profile (2001). Planning Commission, Government of India.

Houghton J T, Ding Y, Griggs D J, Noguer M, Van der Linden PJ, Dai X, Maskell K, Johson CA (eds)., 2001. Climate Change 2001:The Scientific Basis. Contribution of Working Group I to the Third Assessment Report of the Intergovernmental Panel on Climate Change (IPCC) Cambridge University Press, Cambridge, UK.

Houze Jr., R A (2012) Orographic effects on precipitating clouds. Reviews of Geophysics 50, RG1001. DOI: 10.1029/2011RG000365.

Huang Y, Chen S, Cao Q, Hong Y, Wu B, Huang M, Qiao L, Zhang Z, Li Z, Li W and Yang X (2013) Evaluation of Version-7 TRMM Multi-Satellite Precipitation Analysis Product during the Beijing Extreme Heavy Rainfall Event of 21 July 2012. Water 2014, 6, 32-44. DOI: 10.3390/w6010032. ISSN 2073-4441.

Hubanks P A, King M D, Platnick S and Pincus R (2008) MODIS Atmosphere L3 Gridded Product Algorithm Theoretical Basis Document. MODIS Algorithm Theoretical Basis Document No. ATBD-

MOD-30 for Level-3 Global Gridded Atmosphere Products (08_D3, 08_E3, 08_M3) (Collection 005 Version 1.1, 4 December 2008).

Huffman G (2013) 3B42 Version 7 Web Description. http://trmm.gsfc.nasa.gov/3b42.html.

Huffman G J and Bolvin D T (May 2014) TRMM and Other Data Precipitation Data Set Documentation. pmm.nasa.gov/sites/default/files/imce/3B42_3B43_doc_V7.pdf

Huffman G J, Bolvin D T, Nelkin E J and Adler RF (2010) Highlights of Version 7 TRMM Multi-satellite Precipitation Analysis (TMPA). In Proceedings of the 5th International Precipitation Working Group Workshop, Hamburg, Germany, 11–15 October 2010.

IPCC 2007. IPCC Fourth Assessment Report: Climate Change 2007. Solomon, S., D. Qin, M. Manning, Z. Chen, M. Marquis, K.B. Averyt, M. Tignor and H.L. Miller (eds.). Contribution of Working Group I to the Fourth Assessment Report of the Intergovernmental Panel on Climate Change, 2007. Cambridge University Press, UK.

Jamandre C A and Narisma G T (2013) Spatio-temporal validation of satellite-based rainfall estimates in the Philippines. Atmospheric Research 122 (2013) 599–608. DOI:10.1016/j.atmosres.2012.06.024.

Jarvis A, Rubiano J, Nelson A, Farrow A and Mulligan M (2004) Practical use of SRTM data in the tropics: Comparisons with digital elevation models generated from cartographic data. Cali, CO: Centro Internacional de Agricultura Tropical (CIAT), August 2004. 32 p. (Working document no. 198). http://srtm.csi.cgiar.org/PDF/Jarvis4.pdf

Javanmard S, Yatagai A, Nodzu M I, BodaghJamali J and Kawamoto H (2010) Comparing High-Resolution Gridded Precipitation Data with Satellite Rainfall Estimates of TRMM_3B42 over Iran. Advances in Geoscience 25, 119–125. DOI: 10.5194/adgeo-25-119-2010.

Joshi U R and Rajeevan M (2006) Trends in Precipitation Extremes over India. National Climate Centre Research Report No: 3/2006.

Karl T R and Easterling D R (1999) Climate Extremes: Selected Review and Future Research Directions. Climate Change 42: 309-325.

Kelkar R R (2007) Satellite meteorology. B S Publications ISBN: 81-7800-137-3.

Kidder S Q and Vonder Haar T H (1995) Satellite Meteorology An introduction, Academic Press, ISBN: 0-12-406430-2

Khlebnikova E.I. High-Altitude Climate Zones and Climate Types. Gruzaayloa G V (eds.). Environmental Structure and Function: Climate System – Vol. II (2009) ISBN: 978-1-84826-289-8. UNESCO-Encyclopedia of Life Support Systems (EOLSS).

Klein Tank A M G, Zwiers F W and Zhang X (2009) Guidelines on analysis of extremes in a changing climate in support of informed decisions for adaptation. Climate Data and Monitoring WCDMP-72, WMO-TD/No. 1500, June 2009.

Krishnamurthy C K B, Lall U and Kwon H (2009) Changing Frequency and Intensity of Rainfall Extremes over India from 1951 to 2003. Journal of Climate 22(18):4737-4746. DOI: 10.1175/2009JCLI2896.1

Lensky I M and Levizzani V (2008), Estimation of precipitation from space-based platforms, Precipitation: Advances in Measurement, Estimation and Prediction, Silas Michaelides, Springer Publications, ISBN: 978-3-540-77655-0, Pages 195-217.

Leh.nic.in. Accessed on: Jan 2, 2015

Li X, Zhang Q and Chong-Yu X (2013) Assessing the performance of satellite-based precipitation products and its dependence on topography over Poyang Lake basin. Theoretical and Applied Climatology (2014) 115:713–729. DOI 10.1007/s00704-013-0917-x.

Liu G (2003) Determination of Cloud and Precipitation Characteristics in the Monsoon Region Using Satellite Microwave and Infrared Observations. Mausam (India), 54 (2003)51.

Malik N, Bookhagen B, Marwan N and Kurths J (2011) Analysis of spatial and temporal extreme monsoonal rainfall over South Asia using complex networks. Climate Dynamics 39(3-4):971-987. DOI: 10.1007/s00382-011-1156-4

May W (2004) Variability and extremes of daily rainfall during the Indian summer monsoon in the period 1901–1989. Global and Planetary Change 44 (2004) 83–105. DOI: 10.1016/j.gloplacha.2004.06.007.

Nandargi S and Dhar O N (2011) Extreme Rainfall events over the Himalayas between 1871 and 2007. Hydrological Sciences Journal – Journal des Sciences Hydrologiques. 56(6):930-945. DOI: 10.1080/02626667.2011.595373.

Nandargi S and Dhar O N (2012) Extreme Rainstorm Events over the Northwest Himalayas during 1875 – 2010. Journal of Hydrometeorology Vol. 13, 1383–1388. DOI: 10.1175/JHM-D-12-08.1.

Nasrollahi N (2015) Improving Infrared-Based Precipitation Retrieval Algorithms Using Multi-Spectral Satellite Imagery, Springer Theses. DOI 10.1007/978-3-319-12081-2_3.

National Space Development Agency of Japan (NASDA) Earth Observation Center (Feb 2001) TRMM Data Users Handbook. www.eorc.jaxa.jp/TRMM/document/text/handbook_e.pdf

Pai D S, Sridhar L, Rajeevan M, Sreejith O P, Satbhai N S and Mukhopadhyay B (2014) Development of a new high spatial resolution (0.25° × 0.25°) Long Period (1901-2010) daily gridded rainfall data set over India and its comparison with existing data sets over the region. Mausam, 65, 1 (January 2014), 1-18.

Palazzi E, Hardenberg J V and Provenzale A (2013) Precipitation in the Hindu-Kush Karakoram Himalaya: Observations and future scenarios. Journal of Geophysical Research: Atmospheres. Vol. 118, 85–100, DOI: 10.1029/2012JD018697.

Pant G B and Kumar K R (1997) Climates of South Asia. John Wiley & sons. ISBN: 0-471-94948-5.

Paula A and Lettenmaier P (1994) Dynamic Modelling of Orographically Induced Precipitation. Reviews of Geophysics, Vol. 32, 3/ August 1994. Pages 265-284, Paper number 94RG00625.

Petty G W and Krajewski W F (1996) Satellite estimation of precipitation over land. Mjémhgical Sdemes - Jommal- As Sdmces Mjémhgiqmes 41(4) August 1996, 433-452.

Precipitation — GES DISC Goddard Earth Sciences Data and Information Services Center. http://disc.sci.gsfc.nasa.gov/additional/faq/precipitation_faq.shtml. Accessed on: October 28, 2014.

Preethi B, Revadekar J V and Kripalani R H (2011) Anomalous behaviour of the Indian summer monsoon 2009. Journal of Earth System Science 120, No. 5, October 2011, pp. 783–794.

Punay J P and Perez G J P (2014) Evaluation of Modis Cloud Product-Derived Rainfall Estimates. Asian Association of Remote Sensing Proceedings 03, 1–5.

Raina A N (1971) Geography of Jammu and Kashmir, National Book Trust. New Delhi, India.

Rakhecha P R and Soman M K (1994) Trends in the Annual Extreme Rainfall Events of 1 to 3 Days Duration over India. Theoretical and Applied Climatology 237, 227–237.

Rajeevan M, Bhate J and Jaswal A K (2008a) Analysis of variability and trends of extreme rainfall events over India using 104 years of gridded daily rainfall data. Geophysical Research Letters 35:L18707, DOI: 10.1029/2008GL035143.

Rajeevan M, Gadgil S and Bhate J (2008b) Active and Break Spells of the Indian Summer Monsoon. NCC Research Report. NCC 7 March 2008.

Rautela P (2013) Lessons learnt from the Deluge of Kedarnath, Uttarakhand, India. Asian Journal of Environment and Disaster Management 5, 43–51. DOI: 10.3850/S1793924013002824.

Rosenfeld D (2007) Cloud Top Microphysics as a Tool for Precipitation Measurements. In: Measuring precipitation from space – EURAINSAT and the future. V. Levizzani, P. Bauer, and F. J. Turk (eds), Springer, 61–78.

Sapiano M R P and Arkin P A (2009) An Intercomparison and Validation of High-Resolution Satellite Precipitation Estimates with 3-Hourly Gauge Data. Journal of Hydrometeorology Vol. 10, 149–166. DOI: 10.1175/2008JHM1052.1.

Sen Roy S (2009) A Spatial Analysis of Extreme Hourly Precipitation Patterns in India. International Journal of Climatology. 29: 345–355 (2009). DOI: 10.1002/joc.1763.

Sen Roy S and Balling R C (2004) Trends in Extreme Daily Precipitation Indices in India. International Journal of Climatology 24: 457–466 (2004). DOI: 10.1002/joc.995.

Shepard D (1968) A two-dimensional interpolation function for irregularly spaced data", Proc. 1968 ACM Nat. Conf, 517-524.

Shrestha M L (2000) Interannual Variation of Summer Monsoon Rainfall over Nepal and Its Relation to Southern Oscillation Index. Meteorology and Atmospheric Physics, 75, 21-28. DOI: 10.1007/s007030070012.

Shrestha D, Singh P and Nakamura K (2012) Spatiotemporal variation of rainfall over the central Himalayan region revealed by TRMM Precipitation Radar. Journal of Geophysical Research: Atmospheres 117, D22106, DOI: 10.1029/2012JD018140.

Singh P and Kumar N (1997) Effect of Orography on Precipitation In The Western Himalayan Region. Journal of Hydrology 199 (1997) 183-206.

Singh R B and Mal S (2014) Trends and Variability of Monsoon And Other Rainfall Seasons in Western Himalaya, India. Atmospheric Science Letters 15, 218–226. doi:10.1002/asl2.494.

Smith R B (1979) The Influence of Mountains on the Atmosphere. Advances in Geophysics, Vol. 21. ISBN: 0-12-018821-X.

Smith R B (1982) A Differential Advection Model of Orographic Rain. Mon Wea Rev 110, 306-310, 1982.

Smith T M, Arkin P A, Bates J J and Huffman G J (2006) Estimating Bias of Satellite-Based Precipitation Estimates. Jounal of Hydrometeorology 7, 841–856.

Sumner G (1988) Precipitation Process and analysis. John Wiley & sons, ISBN: 0-471-90534-8.

Tawde S A and Singh C (2014), Investigation of orographic features influencing spatial distribution of rainfall over the Western Ghats of India using satellite data. International Journal of Climatology. DOI: 10.1002/joc.4146.

Thayyen R J, Dimri A P, Kumar P and Agnihotri G (2013) Study of cloudburst and flash floods around Leh, India, during August 4–6, 2010. Natural Hazards 65, 2175–2204. DOI: 10.1007/s11069-012-0464-2.

Whiteman C D (2000). Mountain meteorology: Fundamentals and Applications. Oxford University Press, Inc. ISBN: 0-19-513271-8.

Wulf H, Bookhagen B and Scherler D (2010) Seasonal precipitation gradients and their impact on fluvial sediment flux in the northwest Himalaya. Geomorphology 118(1-2):13–21. DOI:10.1016/j.geomorph.2009.12.003.

Xie P, Yatagai A, Chen M, Hayasaka T, Fukushima Y, Liu C and Yang S (2007) A gauge-based analysis of daily precipitation over East Asia. Journal of Hydrometeorology 8, 607–626. DOI: 10.1175/JHM583.1.

Zulkafli Z, Buytaert W, Onof C, Bastianmanz, Tarnavsky E, Lavado W and Guyot J (2014) A Comparative Performance Analysis of TRMM 3B42 (TMPA) Versions 6 and 7 for Hydrological Applications over Andean – Amazon River Basins. Journal of Hydrometeorology 15, 581-592. DOI: 10.1175/JHM-D-13-094.1.

APPENDICES

Appendix I: The Python and MATLAB scripts for the extraction of TRMM 3B42 v7 files and creation of 8 time-step files

```
# This program extracts HDF file from the archive file using 7-zip
# application. This program is written for extraction of TRMM 3B42 V7
# data only. This script has been written by Vidhi Bharti, MSc NHDRM
# (2013-15) on October 10, 2014.

import os,glob
path=r'E:\trmmv7'
years=range(1998,2014)
days=range(1,367)
for i in years:
    for j in days:
        if j<10:
            datapath=path+'\\'+str(i)+'\\'+'00'+str(j)
        elif j>9 and j<100:
            datapath=path+'\\'+str(i)+'\\'+'0'+str(j)
        else:
            datapath=path+'\\'+str(i)+'\\'+str(j)
        if os.path.exists(datapath)==False:
            continue
        else:
            os.chdir(datapath)
            for file in glob.glob('*.Z'):
                command='7z e '+file
                x=os.system(command)
                if x!=0:
                    print 'error extracting '+file
```

****

This program utilizes TRMM 3B42 V7 3-hourly data. It creates 8 time-step files for 0,3,6,9,12,15,18,21 time steps respectively for all the years. The data is extracted for JJAS months over Northwest Himalaya region extending from 28 to 37 degrees N and 72 to 82 degrees E. This script has been written by Vidhi Bharti, MSc NHDRM (2013-15) on October 17, 2014.

****

```
clear all
close all
f=fopen('F:\trmmv7\trmm3b42v7.txt');
time_00=0;
time_03=0;
time_06=0;
time_09=0;
time_12=0;
time_15=0;
time_18=0;
time_21=0;
while ~feof(f)
    tline=fgetl(f);
    str=regexp(tline,'\\','split');
```

```
    day=str2num(cell2mat(str(4)));
    if day>=152 & day<=273
        precipitation=hdfread(tline,'precipitation');
        precipitation=precipitation([1009:1049],[313:349]);
        precipitation(precipitation<0)=0;
        precipitation=3*precipitation;
        [pathstr,name,ext]=fileparts(tline);
        newfile=regexp(name,'[^.]+','match');
        file_time=newfile(3);
        file_time=cell2mat(file_time);
        file_date=newfile(2);
        file_date=cell2mat(file_date);
        if file_time=='00'
            time_00=time_00+precipitation;
        end
        if file_time=='03'
            time_03=time_03+precipitation;
        end
        if file_time=='06'
            time_06=time_06+precipitation;
        end
        if file_time=='09'
            time_09=time_09+precipitation;
        end
        if file_time=='12'
            time_12=time_12+precipitation;
        end
        if file_time=='15'
            time_15=time_15+precipitation;
        end
        if file_time=='18'
            time_18=time_18+precipitation;
        end
        if file_time=='21'
            time_21=time_21+precipitation;
        end
    end
end
fclose(f);
```

Appendix II: Rainfall distribution plots for the list of cloudburst events mentioned in the table 5.1

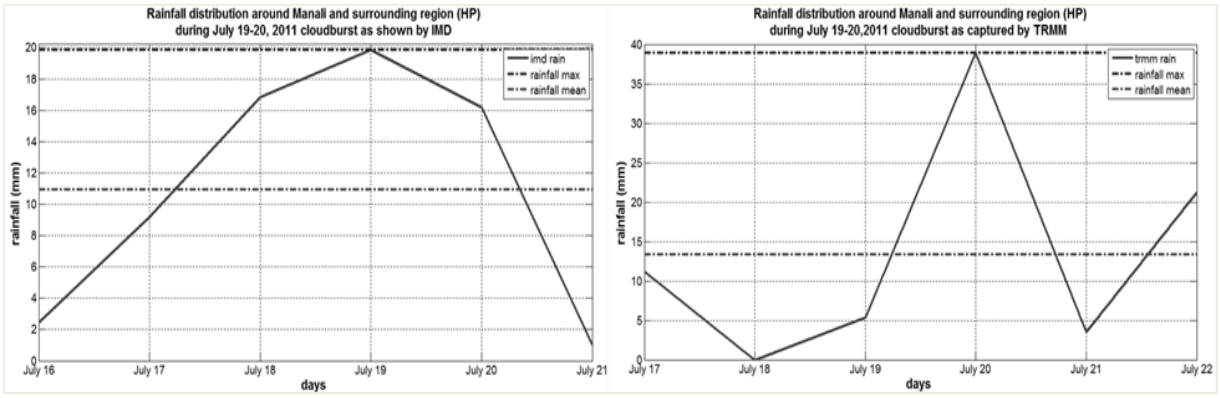

Figure a: Rainfall distribution around Rohtang La (Manali) and nearby regions during cloudburst event on July 19-20, 2011 as captured by (a) IMD data (b) TRMM data

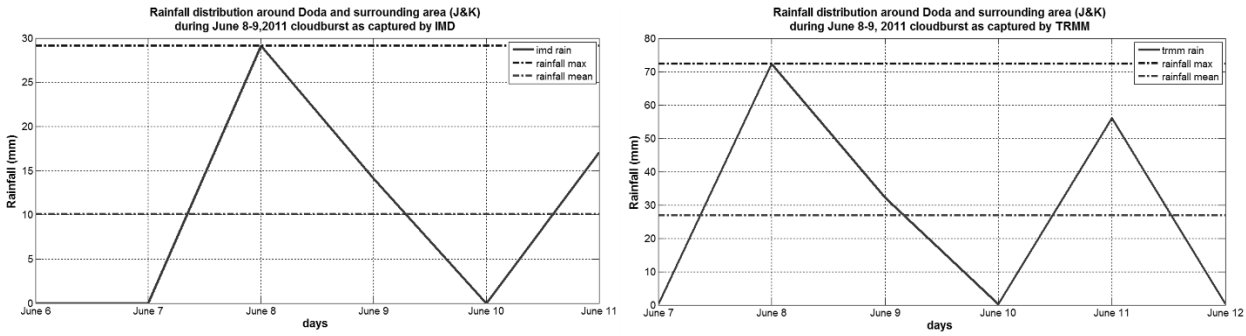

Figure b: Rainfall distribution around Doda and nearby regions during cloudburst event on June 8-9, 2011 as captured by (a) IMD data (b) TRMM data

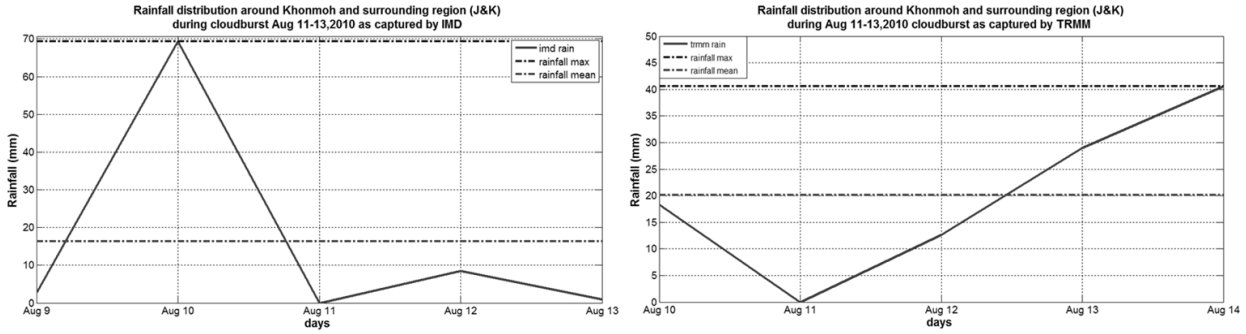

Figure c: Rainfall distribution around Khonmoh and nearby regions during cloudburst event on Aug 11-13, 2010 as captured by (a) IMD data (b) TRMM data

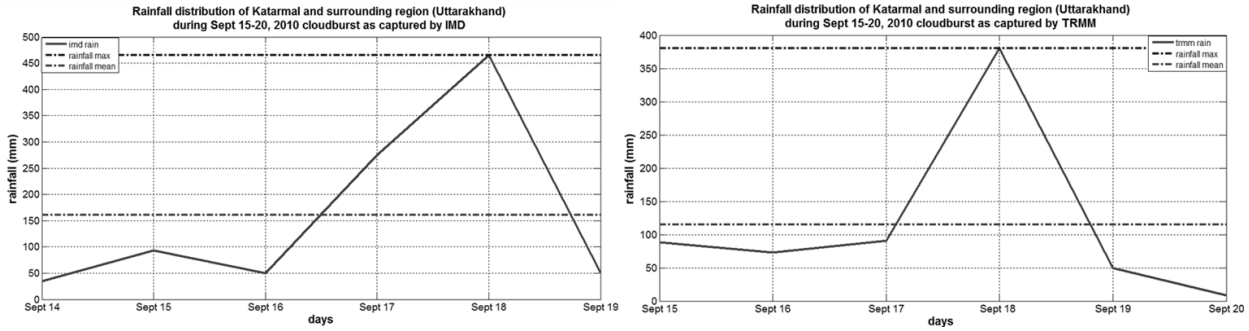

Figure d: Rainfall distribution around Katarmal and nearby regions during cloudburst event on Sept 15-20, 2010 as captured by (a) IMD data (b) TRMM data

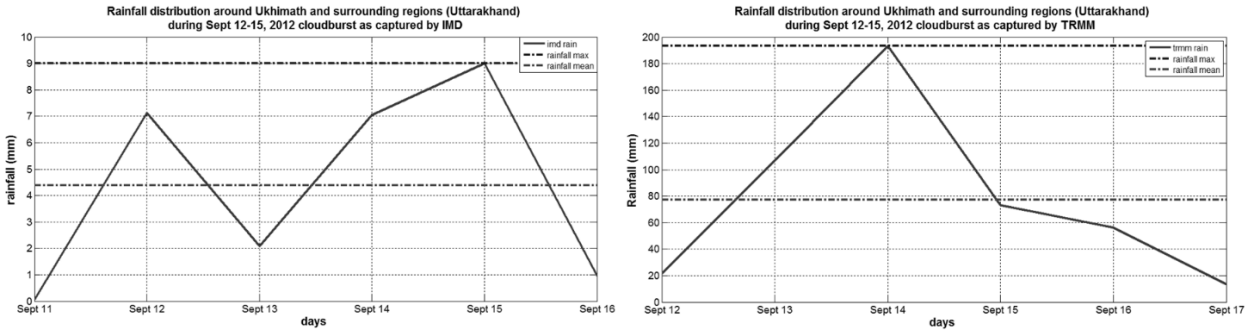

Figure e: Rainfall distribution around Ukhimath and nearby regions during cloudburst event on Sept 12-15, 2012 as captured by (a) IMD data (b) TRMM data

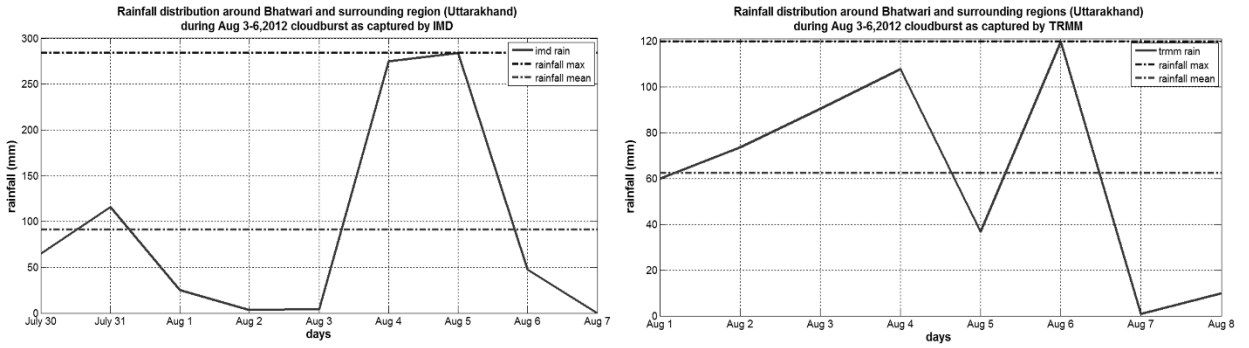

Figure f: Rainfall distribution around Bhatwari and nearby regions during cloudburst event on Aug 3-6, 2012 as captured by (a) IMD data (b) TRMM data

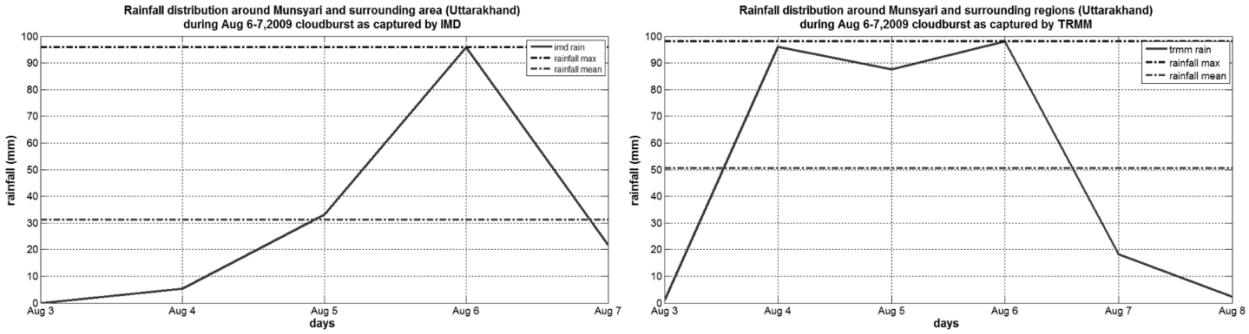

Figure g: Rainfall distribution around Munsyari and nearby regions during cloudburst event on Aug 6-7, 2009 as captured by (a) IMD data (b) TRMM data

Appendix III: Percentile plots for the northwest Himalaya region

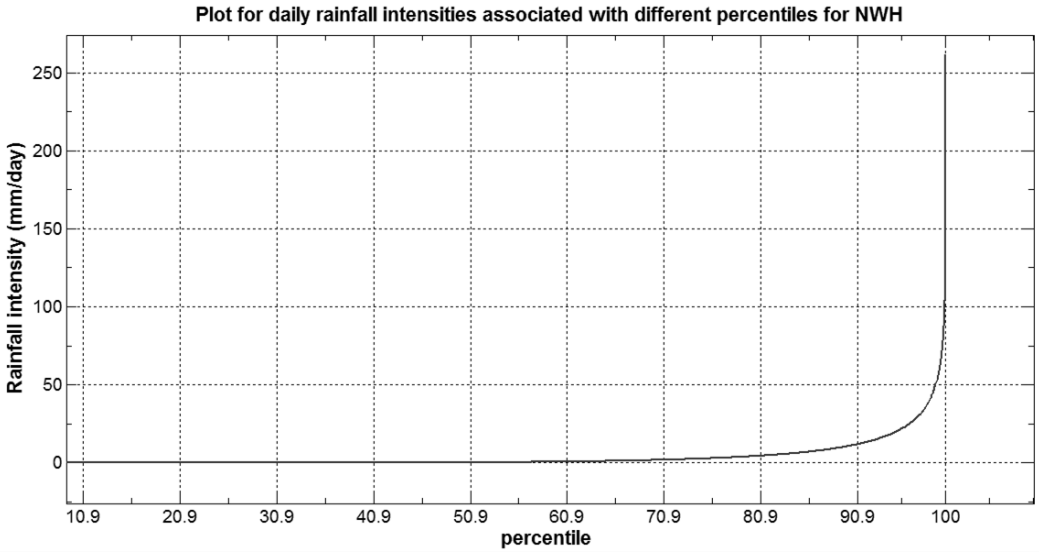

Figure h: Plot depicting rainfall intensity associated with different percentiles over NWH using 16 years of TRMM data

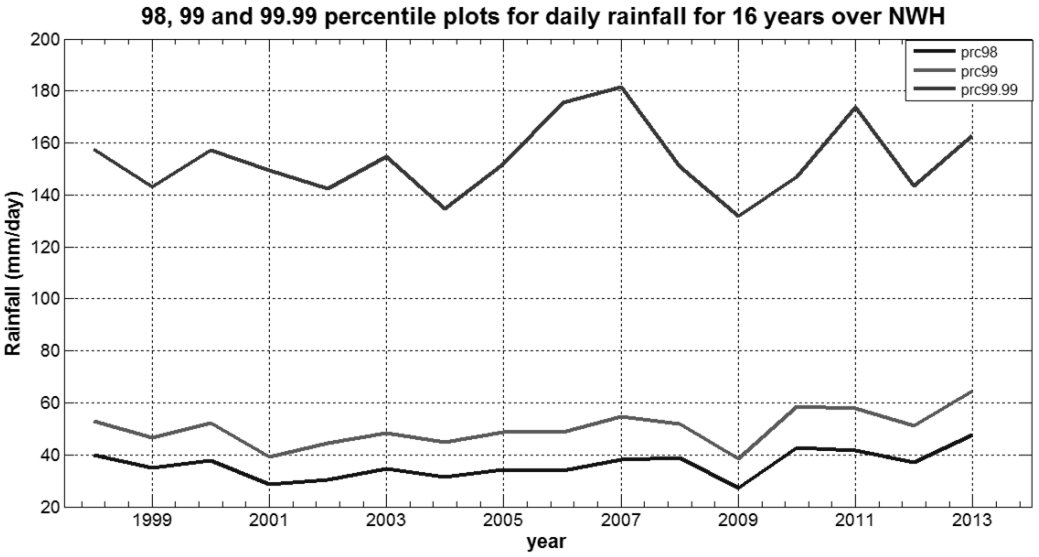

Figure i: 98th, 99th and 99.99th percentile plots for monsoon season NWH using 16 years of TRMM data

Appendix IV: Mean monsoonal rainfall distribution in the Northwest Himalaya

In order to understand the spatiotemporal distribution of EREs, it is imperative to first acquaint with the spatiotemporal rainfall distribution in the region. As the region is highly mountainous, previous studies have shown that Himalayan foothills receive maximum rainfall and the amount of rainfall decreases as one proceeds northwards towards higher elevations (Nandargi and Dhar 2011 and references therein). The mean monsoonal rainfall derived by TRMM has been shown in the figure 5.3. It shows that the maximum daily rainfall occurs in southeast of the NWH in Uttarakhand state with 12-14 mm day^{-1} while the lowest rainfall has been noticed in high altitude regions of leeward side of the Himalayas in J&K state with intensity even less than 1 mm day^{-1}. Below 3000 m elevation the rainfall ranges between 6 to 18 mm day^{-1}.

The mean monsoonal rainfall also varies within the NWH region. The regional distribution shows that in HP and UT, the Southeast and Northwest regions have highest mean monsoonal rainfall. In J&K, the southwest regions have high mean monsoonal rainfall. Altogether, mean monsoonal precipitation decreases gradually with increasing elevation in all the states. In J&K, the district of Kathua has highest mean seasonal rainfall with 8.70 mm day^{-1} out of all the regions while Ladakh (0.37 mm day^{-1}) has the lowest. The districts of Champawat (12.33 mm day^{-1}), Pithoragarh (12.19 mm day^{-1}) and Dehradun (11.29 mm day^{-1}) in Uttarakhand have high mean monsoonal rainfall. The district of Kangra with 11.53 mm day^{-1} in HP has maximum mean seasonal rainfall out of all the districts.

In order to check the trend for mean monsoonal rainfall intensity, the area-averaged plots for mean monsoonal rainfall for past 16 years were plotted. To find whether the slope of regression line is significantly different than zero, student's t-test was performed. The null hypothesis states that the slope is zero i.e. there's no trend present and the alternate hypothesis states that the slope is not equal to zero i.e. some trend is present.

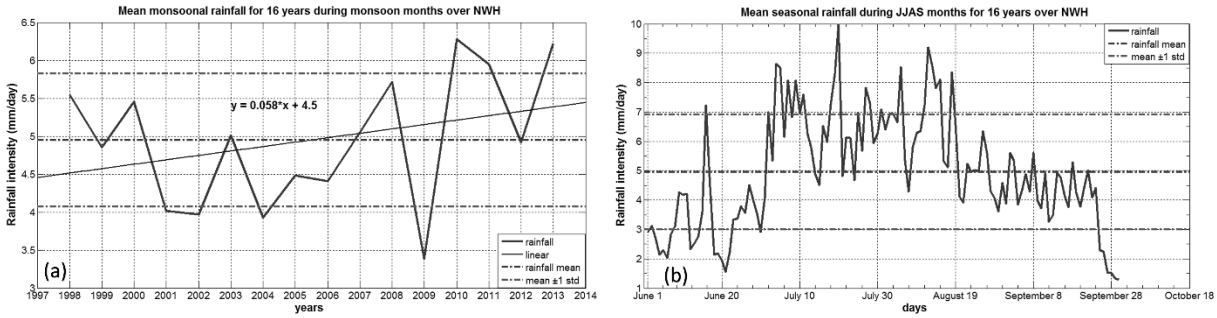

Figure j: Mean seasonal rainfall plots for monsoon season from 1998-2013 over NWH
(a) Inter-annual plot (b) seasonal plot

The test result for inter-annual plot indicates that the slope is significant even at 1% significance level ($p \sim 0$). This indicates that mean monsoonal rainfall is increasing over the years. Mostly the oscillations are well within the ±1 standard deviation limits of mean suggesting that there may be regional factors responsible for such trend rather than external factors. The year 2009 was the most severe monsoon drought year for Indian subcontinent since year 1972 (Preethi *et al*. 2011) which is evident as a large dip in the inter-annual plot. Further, the state-wise plots for mean monsoonal rainfall for past 16 years also showed increasing trend for all three states with Uttarakhand having the steepest positive slope of regression line. The trend has been found significant even at 1% significance level. Previous studies showed different results at state level. Basistha *et al*. (2009) observed decreasing trend of rainfall on Uttarakhand state over the period of 1901 – 1980 using IMD data whereas Singh and Mal (2014) saw no definite pattern over the state after assessing IMD data. Guhathakurta and Rajeevan (2006) with the help of IMD data saw increasing trend in monsoonal rain over J&K. Increasing trend of monsoon rainfall using IMD data has been observed in Himachal Pradesh (Basistha *et al*. 2009 and references therein).

The figure (j) also shows the seasonal rainfall variation (right panel) of mean monsoonal rainfall (mm day^{-1}) for all grid points of NWH. It shows that the high and low peaks are not continuous but vary throughout the period. This is due to the fact that monsoon strength is not uniform throughout the season. The intra-seasonal variation is caused by active and break spells of the monsoon (the movement of ITCZ) which are sporadic and unpredictable phenomena. The peaks start increasing gradually from July 1st (the official monsoon onset date for UT). From then on the high peaks of rainfall can be observed till August, this is when the monsoon is at its full strength. After mid-August, the peaks drop down gradually as the withdrawal period of the monsoon approaches. One anomaly here is the high peak observed on June 16. The reason is the exceptional high rainfall received on June 16, 2013 which was a never-seen-before event during June month for the past 16 years, also responsible for the Kedarnath disaster. For the recorded rainfall intensity during the disaster, please refer Table 5.1.

Appendix V: Correlation analysis between elevation and mean seasonal rainfall over NWH and the states of Uttarakhand, Himachal Pradesh and Jammu & Kashmir

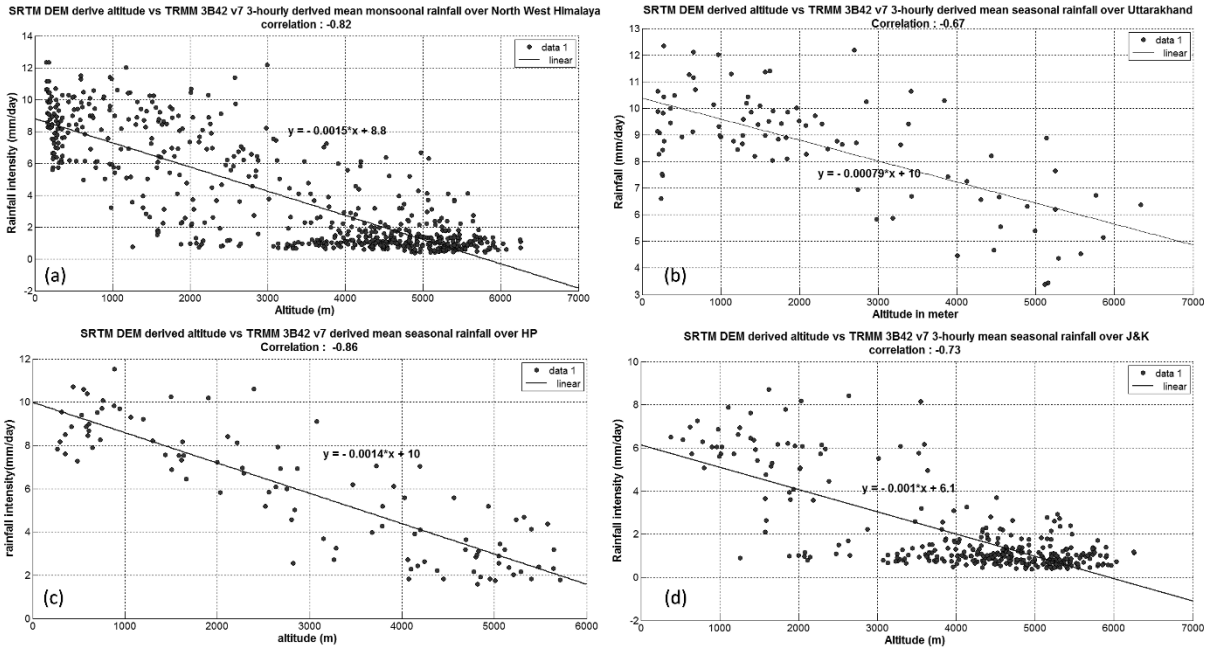

Figure k: Correlation analysis between SRTM DEM derived elevation and TRMM 3B42 v7 derived mean seasonal rainfall over (a) Northwest Himalaya region (b) Uttarakhand region (c) Himachal Pradesh region (d) Jammu & Kashmir region

Appendix VI: Movement of rain bands prior and after Kedarnath event

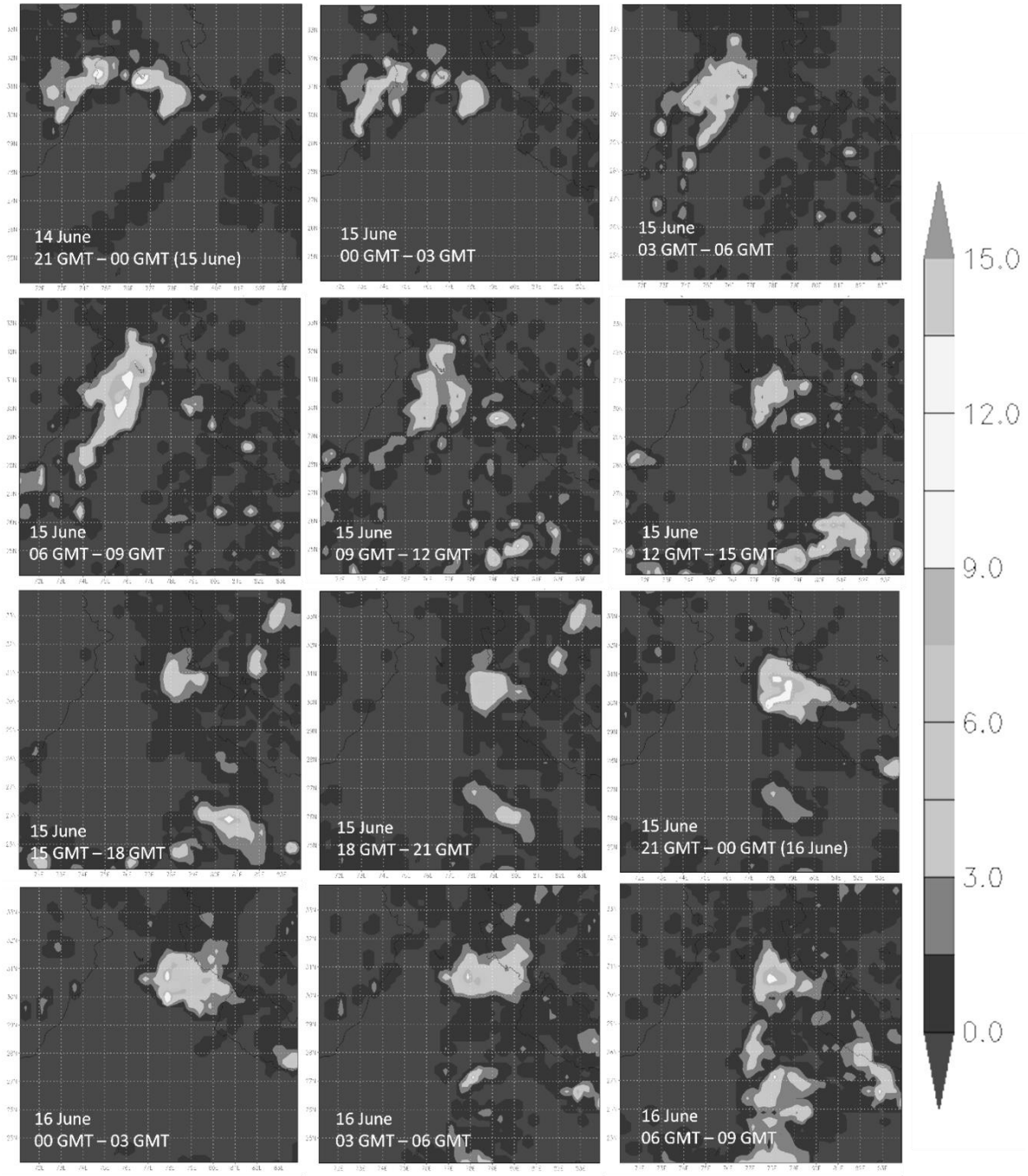

(continued..)

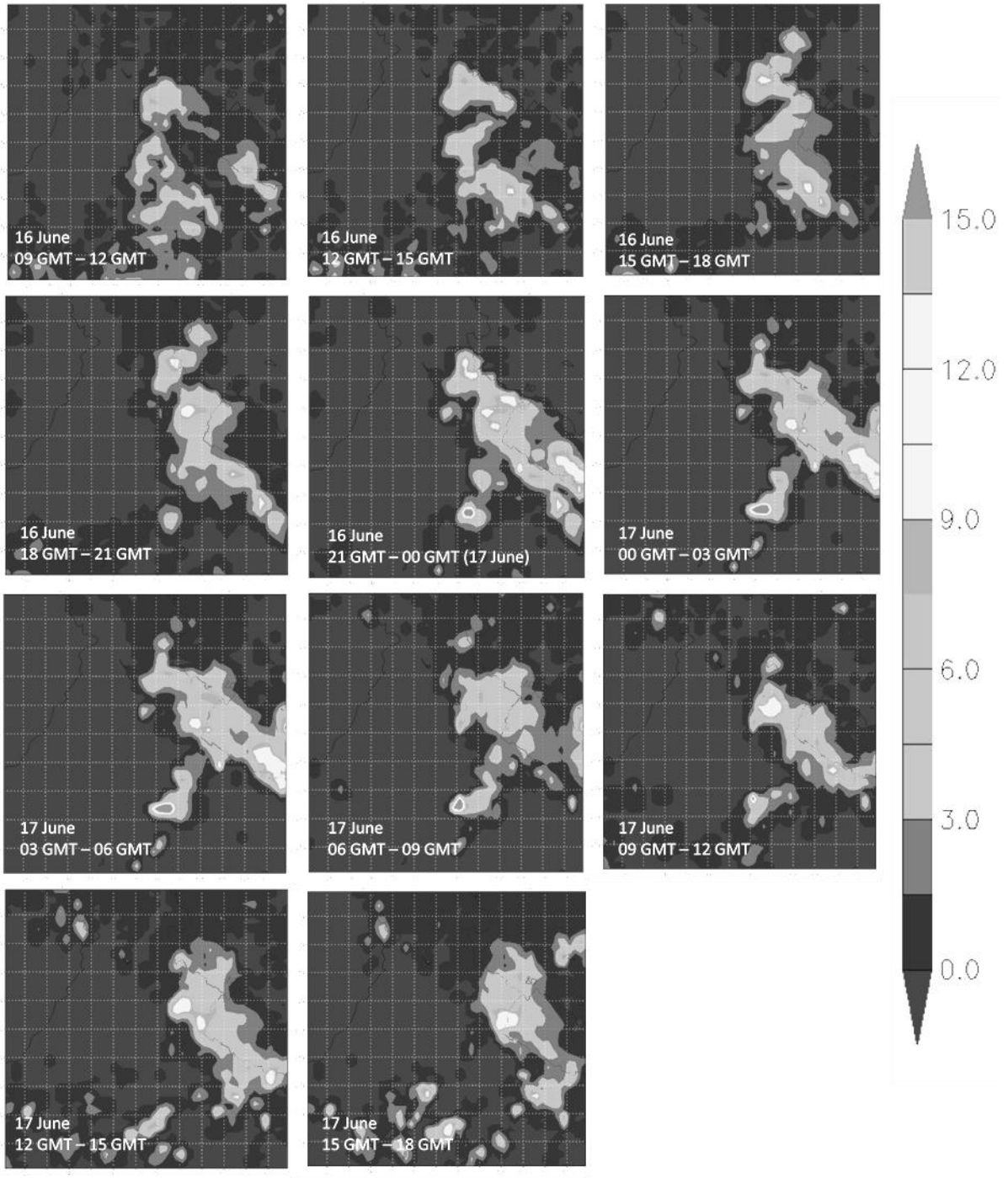

Figure l: Movement of rain bands during the multi-date Kedarnath event. The left top corner image corresponds to 14 June, 2013 from 21 GMT. The map are plotted for 3-hour temporal resolution. The colour bar indicates the rainfall intensity in mm/h

Appendix VII: International Satellite Cloud Climatology Project (ISCCP) derived cloud classification table

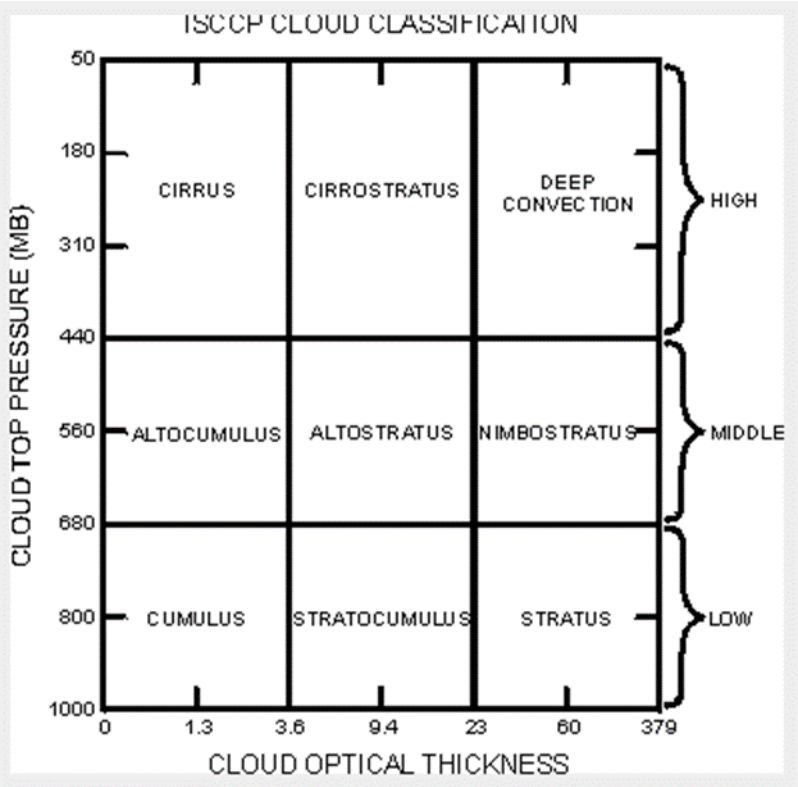

Figure m: ISCCP cloud classification scheme